



HAL
open science

Exploiting the Reactivity of Fluorinated 2-Arylpyridines in Pd-Catalyzed C-H Bond Arylation for the Preparation of Bright Emitting Iridium(III) Complexes

Rabab Boyaala, Marie Peng, Wun-Shan Tai, Rachid Touzani, Thierry Roisnel,
Vincent Dorcet, Yun Chi, Véronique Guerschais, Henri Doucet, Jean-François
Soulé

► To cite this version:

Rabab Boyaala, Marie Peng, Wun-Shan Tai, Rachid Touzani, Thierry Roisnel, et al.. Exploiting the Reactivity of Fluorinated 2-Arylpyridines in Pd-Catalyzed C-H Bond Arylation for the Preparation of Bright Emitting Iridium(III) Complexes. *Inorganic Chemistry*, 2020, 59 (19), pp.13898-13911. 10.1021/acs.inorgchem.0c01528 . hal-03040129

HAL Id: hal-03040129

<https://hal.science/hal-03040129>

Submitted on 4 Dec 2020

HAL is a multi-disciplinary open access archive for the deposit and dissemination of scientific research documents, whether they are published or not. The documents may come from teaching and research institutions in France or abroad, or from public or private research centers.

L'archive ouverte pluridisciplinaire **HAL**, est destinée au dépôt et à la diffusion de documents scientifiques de niveau recherche, publiés ou non, émanant des établissements d'enseignement et de recherche français ou étrangers, des laboratoires publics ou privés.

Exploiting the Reactivity of Fluorinated 2-Arylpyridines in Pd-Catalyzed C–H Bond Arylation for the Preparation of Bright Emitting Iridium(III) Complexes

Rabab Boyaala,^{†,‡} Marie Peng,[†] Wun-Shan Tai,[¶] § Rachid Touzani,[‡] Thierry Roisnel,[†] Vincent Dorcet,[†] Yun Chi,[¶] §* Véronique Guerschais,^{†*} Henri Doucet,^{†*} and Jean-François Soulé^{†*}

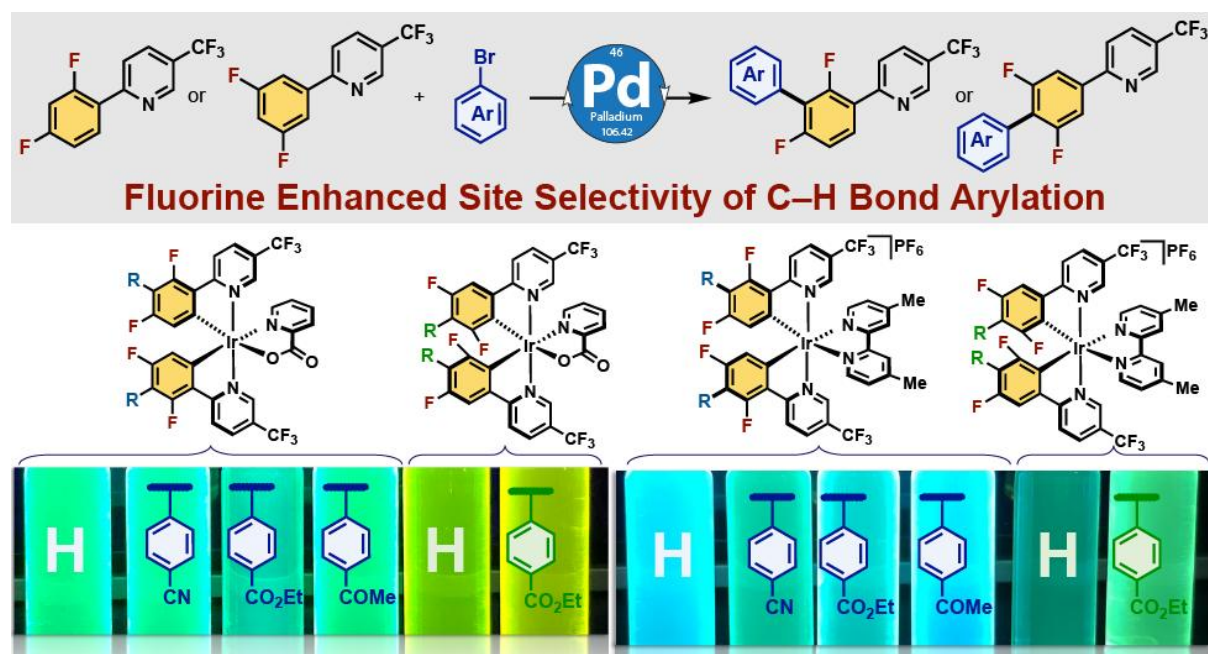
[†] Univ Rennes, CNRS UMR6226, F-3500 Rennes, France.

[‡] Laboratoire de Chimie Appliquée et Environnement (LCAE), Faculté des Sciences, Université Mohamed Premier, Oujda, Morocco.

[¶] Department of Chemistry, National Tsing Hua University, Hsinchu 30013, Taiwan;

§ Department of Materials Science and Engineering, City University of Hong Kong, Hong Kong SAR

KEYWORDS. Catalysis – Palladium – C–H Bond Functionalization – Iridium – Luminescence.



ABSTRACT. Pd-catalyzed C–H bond arylation applied to 2-(2,4-difluorophenyl)-5-(trifluoromethyl)pyridine (**1**) and 2-(3,5-difluorophenyl)-5-(trifluoromethyl)pyridine (**5**) allows the access to two families of Ir(III) complexes, charge-neutral and cationic species.

The reaction is regioselective since only the C3- or C4-position of the fluorinated phenyl ring of **1** or **5** is readily functionalized - namely the C–H bond flanked by the two fluorine atoms which is the most acidic - which allows the electronic control of the reactive site. A range of electron-withdrawing (CN, CO₂Et, C(O)Me) substituents on the aryl group has been incorporated leading to the pro-ligands (Ar-2,4-dFppy; **2**, Ar = *p*-C₆H₄-CN; **3**, Ar = *p*-C₆H₄-CO₂Et; **4**, Ar = *p*-C₆H₄-C(O)Me; and Ar-3,5-dFppy; **6**, Ar = *p*-C₆H₄-CO₂Et). The unsubstituted complexes **F/G-1** and **F/G-5** featuring **1** and **5** respectively, as C^N ligands are used as reference complexes. The families of five charge-neutral [Ir(C^N)₂(N^O)] complexes (C^N is 2-(5-aryl-(4,6-difluorophenyl)-5-(trifluoromethyl)pyridinato (**F2-F4**), and 2-(4-aryl-(3,5-difluorophenyl)-5-(trifluoromethyl)pyridinato (**F5-F6**), N^O = 2-picolinate] and five cationic [Ir(C^N)₂(N^N)]PF₆ complexes [N^N = dmbpy is 4,4'-dimethyl-2,2'-bipyridine] (**G2-G6**) were synthesized and their structural and photophysical properties studied with comparison to the unsubstituted analogues used as reference complexes. The appended aryl group provides large steric bulk as the biaryl fragment is twisted as shown by the X-ray crystal structures of **F2**, **F5**, **F6**, **G3** and **G5**. These latter complexes display a wide variety of different Ir...Ir intermetallic distances in crystals, from 8.150 Å up to 15.034 Å. Moreover, the impact on the emission energy is negligible, as a result of the breaking of the conjugation between the two aryl groups. Charge-neutral complexes [Ir(C^N)₂(N^O)] (N^O = 2-picolinate) show bright luminescence: **F2-F4** (λ_{em} = 495-499 nm) are blue-green emitters whereas **F5** and **F6** (λ_{em} = 537, 544 nm), where the fluorine substituents are located at the C3- and C5-positions, emit in the green region of the visible spectrum. In all cases, a unitary photoluminescence quantum yield is found. The improvement of φ might be explained by an increase of the radiative rate constant due to a higher degree of rigidity of these congested molecules, compared to the unsubstituted complex **F1**. The same trends are observed for the family of complexes **G**. Complexes **G1-G4** exhibit blue photoluminescence, and **G5** and **G6** leads to a red-shifted emission band, as also found for the related complexes **F5** and **F6** due to the similar fluorine substitution pattern. Their emission quantum yields are remarkably high for charged complexes in CH₂Cl₂ solution. These results showed that Pd-catalyzed C–H bond arylation is a valuable synthetic approach for designing efficient emitters with tunable photophysical properties.

INTRODUCTION

The design and synthesis of cyclometalated iridium(III) complexes has focused much interest for their applications in electroluminescent devices due to their intriguing luminescent behavior, *i.e.*, long-lived excited states, high luminescence efficiencies, and facile color's tuning by ligand design.¹ Typically, *bis*-cyclometalated ppy-based (ppyH 2-phenylpyridine) neutral Ir(III) complexes of the type $[\text{Ir}(\text{C}^{\wedge}\text{N})_2(\text{L}^{\wedge}\text{X})]$ (where $\text{C}^{\wedge}\text{N}$ and $\text{L}^{\wedge}\text{X}$ are cyclometalated ligand and monoanionic ancillary) were employed as dopants in organic light-emitting diodes (OLEDs),² while their cationic congeners $[\text{Ir}(\text{N}^{\wedge}\text{C})_2(\text{N}^{\wedge}\text{N})]\text{PF}_6$ ($\text{N}^{\wedge}\text{N}$ is a di-imine ligand) were used in light-emitting electrochemical cells (LEECs).³

A plethora of charge-neutral and cationic phosphorescent Ir-ppy based complexes displaying emission ranging from red to blue have been reported to date, their synthesis and photophysical properties being well-documented in the literature.⁴ Numerous chemical modifications allowing the control of the emission energy have been reported. For instance, in the case of the neutral iridium(III)*bis*[(4,6-difluorophenyl)-pyridinato-*N,C2'*]picolinate Irpic , **A** (Figure 1), the most studied bis-cyclometalated iridium complex,⁵ introduction of strong electron-withdrawing substituents such as perfluorocarbonyl,⁶ benzoyl⁷ or diphenylphosphoryl⁸ groups (Figure 1, complexes **B–D**) onto the phenyl ring at the C5-position allows to further blue-shift the emission, whereas CF_3 - Irpic ⁹ (**F1**, Figure 1) derivative incorporating an electron-withdrawing substituent at the 5-position of the pyridine ring of dF-ppy displays a bathochromic shift of the emission when compared to the parent unsubstituted complex.

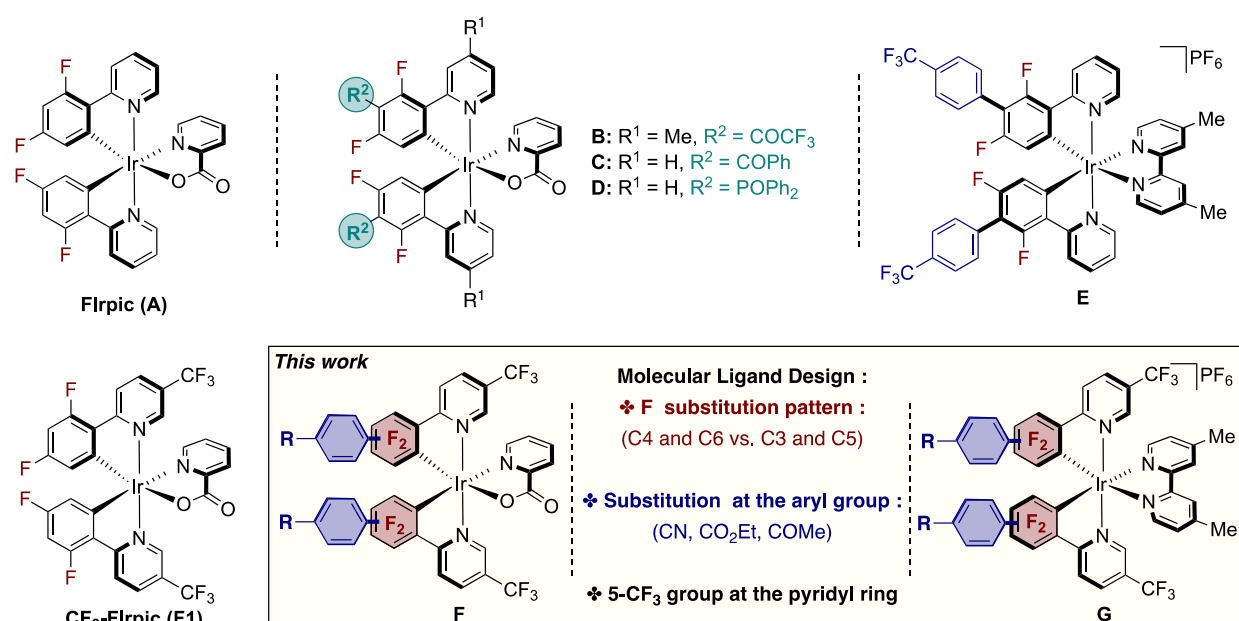


Figure 1. Selected Examples of Cyclometalated Iridium Complexes with difluorinated 2-arylpyridine as C[^]N Ligand and Structure of the Investigated Charge-Neutral and Cationic Iridium Complexes

Adding electron-withdrawing or-donating substituents on the C[^]N ligand is a traditional way to modify the electronic structure of resulting complexes, and hence the color of the emission. On the contrary, the emission energy is not subject to change when adding sterically bulky aryl substituents at the 4-position of the pyridine ring of the C[^]N-ppy ligand, the attainment of a coplanar conformation between the two aromatics is inhibited leading to a disruption of the conjugation.^{3h, 10} This ligand design has been applied for both charge-neutral and cationic bis-cyclometalated complexes, and the decrease of the intermolecular interactions, due to steric hindrance, has led to the most successful complexes with improved device performances. In a synthetic point of view, it is worth-mentioning that in all cases, aryl-appended pro-ligands of dFppyH, were prepared, prior to metal complexation, using classical Suzuki carbon-carbon cross-coupling reactions. To facilitate the access to a large variety of complexes with tunable photophysical properties, we have developed the late-stage modification of fluorinated 2-arylpyridines and 2-arylquinolines, which allowed us to build a library of nitrogen-based pro-ligands in only one-step.¹¹ Our approach was based on regiodivergent metal-catalyzed C–H bond arylations. We showed that in the presence of palladium catalysts, the C–H bond arylation occurred at the adjacent position of the fluorine atoms while using a ruthenium catalyst, the *ortho*-C–H bond of the pyridine or quinoline rings is the selective site of functionalization. Moreover, the corresponding cationic iridium(III) complexes [Ir(C[^]N)₂(N[^]N)]PF₆ featuring these synthesized *p*-CF₃-C₆H₄-appended C[^]N-ligands (see for instance, complex **E**, Figure 1) display an increased photoluminescence quantum yield, compared to the unsubstituted complex.¹¹ Interestingly, the emission band is not affected by this chemical modification, as already observed for the related series of iridium(III) complexes where the substitution is achieved at the 4-position of the pyridyl ring.^{10e, 12} The color of the emission depends on the C[^]N ligand, *i.e.*, the position and number of the fluorine atoms as well as the nature of the nitrogen-based (pyridine or quinoline) ligand. Complex **E** displays a bright luminescence in the green region ($\lambda_{em} = 525$ nm) of the visible spectrum. The nature of the substituent of the incorporated aryl group on the photophysical properties was not investigated at this time, as well as the substitution on the pyridine ring. Only, the *para*-trifluoromethyl-substituted bromo derivative *p*-CF₃-C₆H₄Br was used as the reagent, the first catalytic step of oxidative addition being facilitated, in order

to establish the best catalytic conditions for both Pd and Ru catalytic systems. In order to further explore the scope of this reaction, we decided to investigate Pd-catalyzed C–H bond arylation¹³ of dF-CF₃ppy derivatives using various bromoaryl reagents. Fluorobenzene derivatives are generally very reactive substrates in Pd-catalyzed C–H bond arylation,¹⁴ because fluorine atoms often enhance the reactivity of the adjacent C–H bonds owing to their electronic properties, leading in most cases to site selective reactions.¹⁵ However, 2-(difluorophenyl)-5-(trifluoromethyl)pyridine (dF-CF₃ppyH) derivatives are more challenging substrates in terms of regioselectivity as the presence of the electron-withdrawing 5-trifluoromethyl substituent on the pyridine ring could also enhance the reactivity of the adjacent C–H bond,¹⁶ which could lead to side reactions.

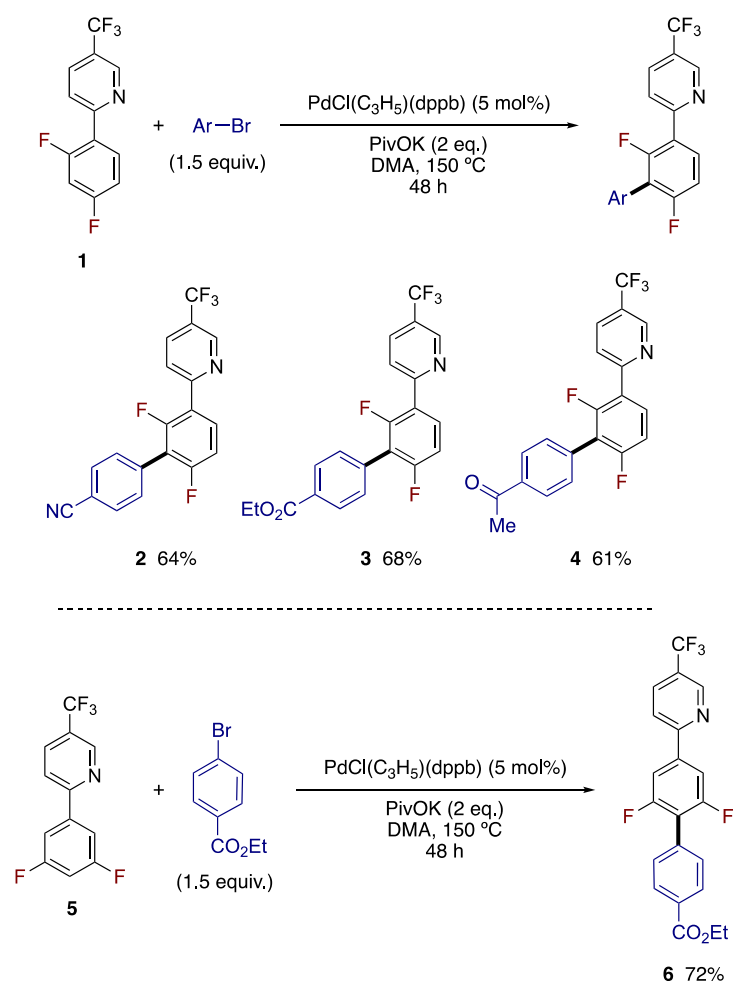
In this report, we extend our catalytic approach to prepare two families of Ir(III) complexes, neutral (**F**⁹) and cationic species (**G**¹⁷) (see Figure 1) containing new aromatically substituted C^N ligands based on 2-(2,4-difluorophenyl)-5-(trifluoromethyl)pyridine (**1**) and 2-(3,5-difluorophenyl)-5-(trifluoromethyl)pyridine (**5**) (Scheme 1), by using regioselective Pd-catalyzed C–H bond arylations. Various aryl groups substituted at the *para*-position by an electron-withdrawing group (CN, CO₂Et, C(O)Me) are readily incorporated, the regioselectivity being electronically controlled by the two fluorine atoms of pro-ligands **1** and **5**.

Herein, we report the synthesis, the X-ray crystal structures, and the solution-state photophysical properties of (i) a family of 2-picolinato complexes of the form [Ir(Ar-dF-CF₃ppy)₂(pic)] **F** and (ii) a series of positively-charged complexes [Ir(Ar-dF-CF₃ppy)₂(dmbpy)]PF₆ **G** having a 4,4'-dimethyl-2,2'-bipyridine ancillary. This will allow us to evaluate the role of the added aryl substituent at the cyclometalated difluorinated phenyl ring of the C^N ligand on the photophysical properties by comparison with the unsubstituted analogues (**F1**⁹ /**F5** and **G1**/**G5**, Schemes 2 and 3) used as reference complexes.¹⁴ We also show that the color of the emission can be fine-tuned by changing the position of the fluorine atoms in both series of complexes (**F1-4** vs. **F5-6** and **G1-4** vs. **G5-6**, see Schemes 2 and 3), from blue to blue-green.

RESULT AND DISCUSSION

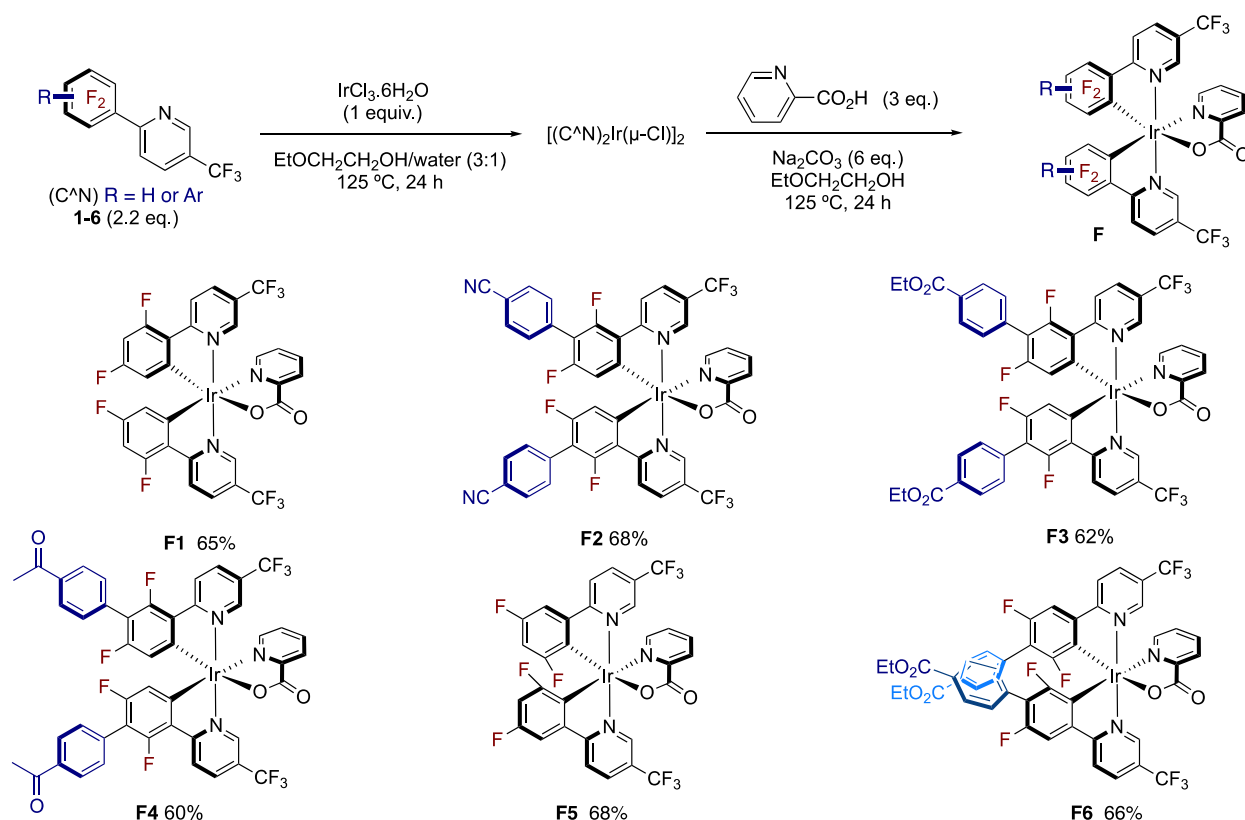
Synthesis. Firstly, we studied the reactivity of 2-(2,4-difluorophenyl)-5-(trifluoromethyl)pyridine (**1**) in palladium-catalyzed C–H bond arylation with 4-bromobenzonitrile as the aryl source (Scheme 1). Using our previous optimized reaction

conditions, namely 5 mol% of PdCl(C₃H₅)(dppb) [dppb = 1,4-bis(diphenylphosphino)butane] associated with 2 equivalents of PivOK as base in DMA at 150 °C, the C–H bond arylation took place regioselectivity on the aryl ring at the most acidic C–H bond, *i.e.* the one flanked by two fluorine atoms, affording the arylated proligand **2** in 64% yield. Other pro-ligands **3** and **4** were prepared using the same procedure from ethyl 4-bromobenzoate and 4-bromoacetophenone in 68% and 61% yield, respectively. We have also investigated the reactivity of 2-(3,5-difluorophenyl)-5-(trifluoromethyl)pyridine (**5**) using ethyl 4-bromobenzoate as coupling partner. Again, the C–H bond arylation under palladium catalysis occurred at the most acidic position to give **6** in 72% as single regioisomer. As we previously observed in the case of 2-(2,4-difluorophenyl)pyridine,¹¹ these phosphine-free palladium conditions are sensitive to the electronic nature of the aryl bromide as only electron-deficient aryl bromides were efficiently coupled owing to their faster rates of the oxidative addition to palladium. However, in all cases, the reaction was very regioselective, affording only the direct arylation at the C–H bond flanked by the two fluorine atoms. These results show that the presence of the 5-CF₃ group on the pyridine ring does not perturb the site selectivity of the catalytic reaction.



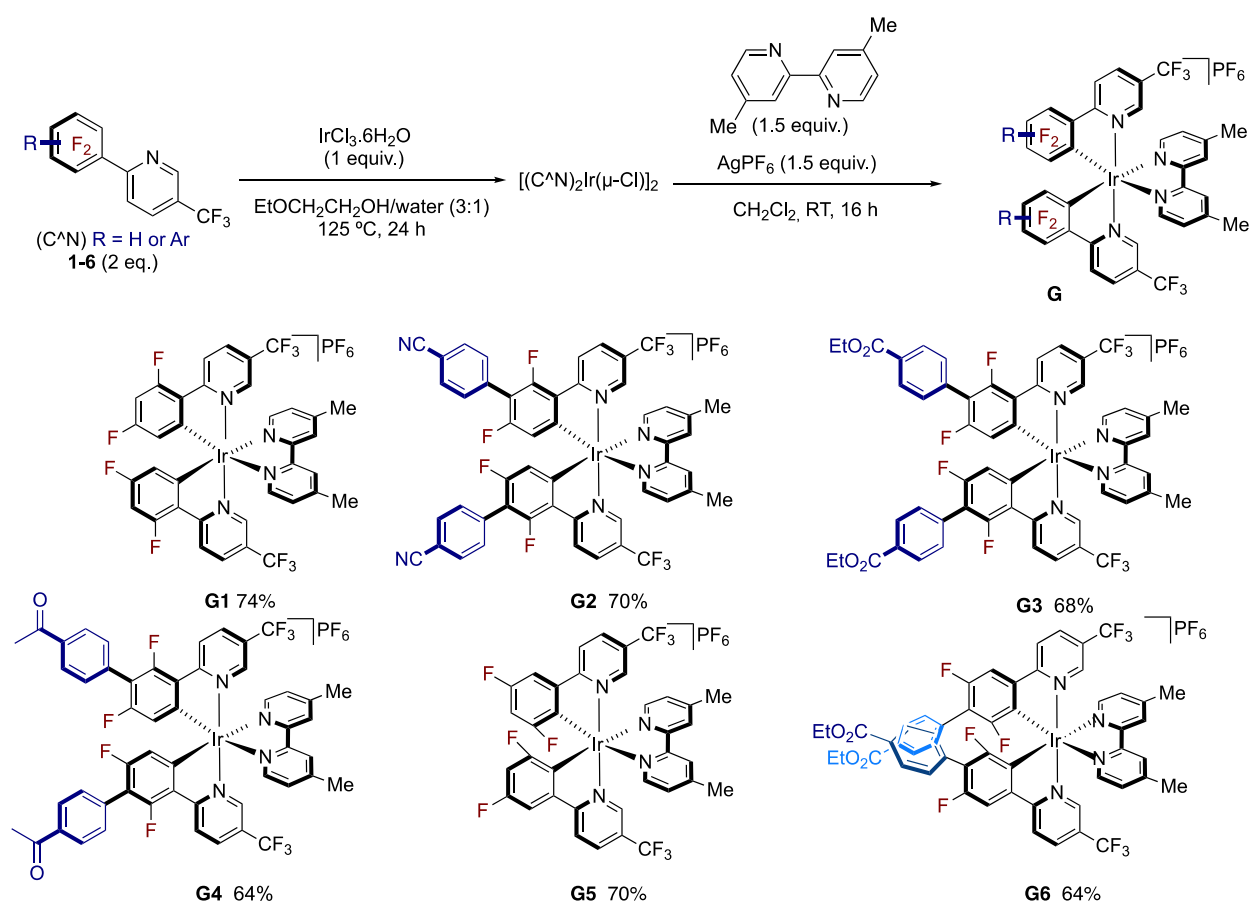
Scheme 1. Pd-Catalyzed C–H Bond Arylation of 2-(2,4-Difluorophenyl)-5-(trifluoromethyl)pyridine (**1**) and 2-(3,5-Difluorophenyl)-5-(trifluoromethyl)pyridine (**5**)

Having synthesized the new pro-ligands **1-6** in pure form *via* Pd-catalyzed C–H bond arylation, we turned our attention to the preparation of charge-neutral iridium(III) complexes **F**, CF₃-Flrpic congeners of **F1** (Scheme 2). The cyclometalated iridium μ -chloro-bridged dimers [(C^{^N})₂Ir(μ -Cl)]₂ were prepared using a classical procedure which consists of a treatment of IrCl₃·3H₂O with **1-6** in a mixture of 2-ethoxyethanol and water at 125 °C for 24h. Then, the crude dimer was treated, without any purification, with 2-picolinic acid in the presence of sodium carbonate in 2-ethoxyethanol at 125 °C over 24h to afford the non-arylated reference complexes **F1**⁹ and **F5** bearing a different difluoro phenyl substituted (4,6-difluorophenyl and 3,5-difluorophenyl, respectively) cyclometalated ligand and the corresponding arylated complexes **F2**, **F3**, **F4** and **F6** featuring a biaryl unit. The novel complexes **F2-F6** were characterized by ¹H-NMR, ¹³C-NMR, and ¹⁹F-NMR spectroscopy and high-resolution mass spectrometry (HRMS) (Synthesis details in SI).



Scheme 2. Preparation of Complexes **F1-F6** with Pyridine-2-carboxylate as Ancillary Ligand

The second family of cationic iridium complexes $[\text{Ir}(\text{C}^{\wedge}\text{N})_2(\text{N}^{\wedge}\text{N})]\text{PF}_6$ (**G**) was prepared using again the fluorinated 2-arylpyridine pro-ligands **1-6**, 4,4'-dimethyl-2,2'-bipyridine being used as the diimine ancillary ligand following the reported two-step procedure (Scheme 3).¹¹ Complexes **G1-G6** were isolated in 64-74% yields as yellow air-stable solids, and were characterized by NMR spectroscopy and high-resolution MALDI mass spectrometry. The complex **G1**, prepared from non-arylated 2-(2,4-difluorophenyl)-5-(trifluoromethyl)pyridine has been previously employed as a catalyst in photocatalytic water reduction, but there was no studies devoted to its luminescent properties.¹⁸



Scheme 3. Preparation of Complexes **G1-G6** with 4,4'-Dimethyl-2,2'-bipyridine as Ancillary Ligand.

X-ray Crystal Structures. Single crystals of **F2**, **F5**, **F6**, **G3**, and **G5** suitable for X-ray analysis were grown by slow diffusion of hexane into a CH_2Cl_2 solution of the respective complexes. The X-ray crystal structures of the neutral complexes **F2**, **F5** and **F6** and the cationic complexes **G3** and **G5** are depicted in Figure 2. Selected bond distances and bond angles as well as selected bite angles are tabulated in Table 1. All complexes, neutral and cationic, exhibited distorted octahedral geometries, with the two $\text{C}^{\wedge}\text{N}$ ligands adopting a C,C-

cis, and N,N-*trans* configuration, similar to that of the archetype complexes.^{4a, 5e} For neutral complexes, the oxygen atom of the picolinate ligand is located *trans* to the C-ligand, as found in the precursor complex **F1**.⁹ The Ir–C and Ir–N bond distances in **F2** are in the same range to those of the unsubstituted complex **F1**. The average Ir–N (2.052 Å) and Ir–C (2.019, Å) bond distances in the C[^]N ligands of **F6** are longer than those observed for the 2-(4,6-difluorophenyl)pyridinato derivatives **F1** and **F2**. The aryl pendant is not coplanar with the C[^]N ligand, the torsion angles between the plane of the incorporated aryl group and that of cyclometalated phenyl ring of the two C[^]N ligands, are 64.30(4)° and 46.20(4)° and 68.20(12)°/61.40(13)° for **F2** and **F6**, respectively. For cationic complexes, the average Ir–Cppy (2.021 Å) and Ir–Nppy (2.053 Å) bond distances of **G5** are elongated, with respect to those in complex **G3**. The added aryl group in **G3** displays a similar twisted conformation observed for **F** series of complexes: the plane of the aryl ring relative to that of the C-connected phenyl displays dihedral angles of 61.30(8)° and 53.00(9)°. Importantly, the distance between two iridium centers for adjacent complexes in the crystal packing varies slightly from 8.150 Å (**F1**)⁹ to 9.044 Å (**F2**) while a more significant increase is observed going from **F5** to **F6**, (9.917 Å to 14.157 Å). Notably, **G3** exhibits the longer intermetallic distance of 15.034 Å, longer than that found for **G5** (10.080 Å) showing the dramatic influence of the presence of the bulky *p*-C(O₂Et)-C₆H₄ group in this case. This distance is significantly greater than to the maximum values reported for the related 4-substituted pyridine cationic complexes which do not exceed 11 Å.¹² These results illustrate the impact of the location (phenyl vs. pyridyl rings of C[^]N-ligands) of the appended aryl group in the solid state.

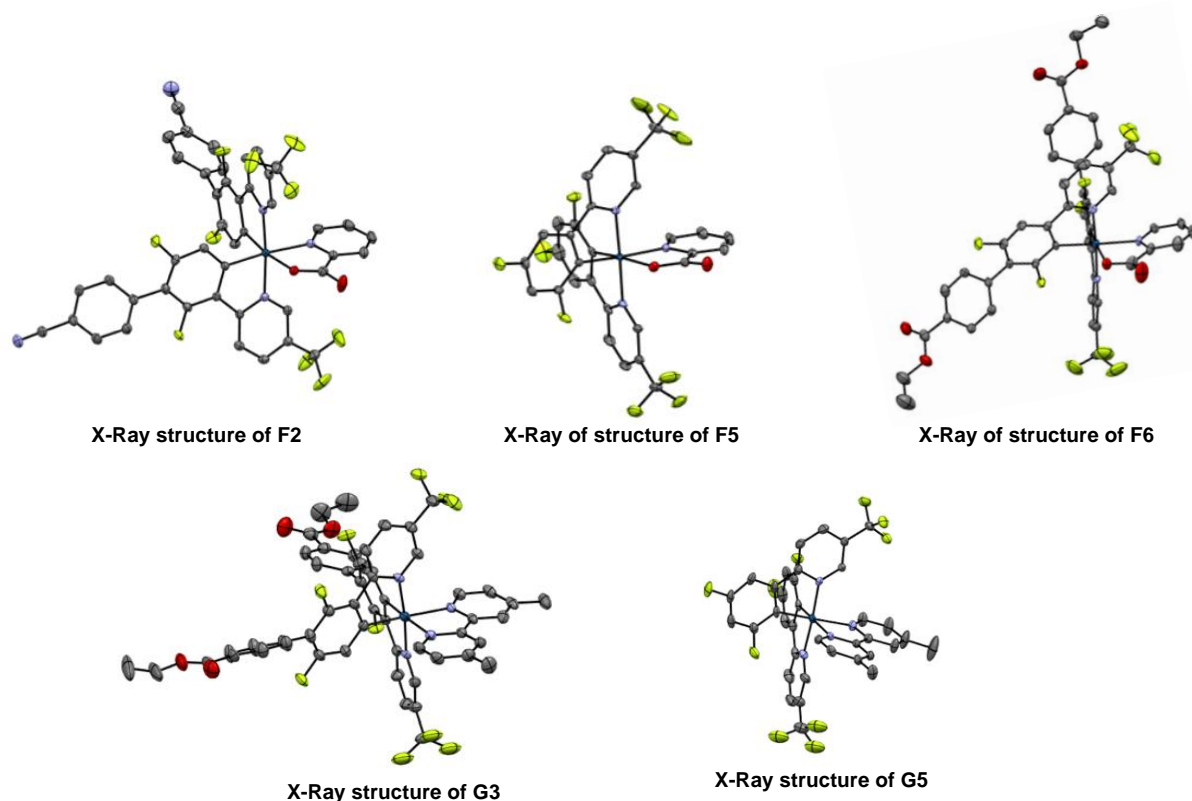


Figure 2. Solid State Structures of Complexes **F2**, **F5**, **F6**, **G3** and **G5**. Hydrogen atoms, solvent and counter anion are omitted for clarity. Thermal ellipsoids are at the 50% probability level.

Electrochemical studies.

The representative voltammograms of complexes **F** and **G** are depicted in Figures S1 and S2, respectively, and the corresponding numerical data are summarized in Table S1 and S2 (see SI). Complexes **F** show irreversible (complexes **F1**, **F3** and **F4**) or quasi-irreversible (complexes **F2**, **F5** and **F6**) oxidation waves in their cyclic voltammograms in CH_2Cl_2 (0.1 M of $n\text{-Bu}_4\text{NPF}_6$ as the supporting electrolyte at a scan rate of 100 mV s^{-1} and using ferrocene/ferrocenium (Fc/Fc^+) as the internal reference). The oxidation waves of **F1-F4** are in the range of +1.08 to + 1.25 V vs. Fc/Fc^+ , which can be attributed to the Ir(III)/(IV) redox couple with contributions from the $\text{C}^{\wedge}\text{N}$ ligands.^{10a} Upon the addition of aryl groups to the 5-position of the phenyl ring, the oxidation waves of **F2-F4** are slightly cathodically shifted, reflecting the moderately increased electron density due to the presence of appended aryl substituents. The irreversible reduction waves are very comparable to one another. The HOMO-LUMO gaps, calculated from these potentials are comparable to that previously found for **F1**.⁹ Both complexes **F5** and **F6** exhibit a quasi-reversible single-electron oxidation wave, a notably less positive oxidation potential than the 4,6-difluoro-based complexes, illustrating the electronic effect of the 3,5-fluorine substitution of the $\text{C}^{\wedge}\text{N}$ ligands

on the anodic potential. The **G** series of Ir(III) metal complexes, which are cationic, display less obvious oxidation peak, due to the reduction of electron density at the metal center compared to the **F** series of charge-neutral metal complexes. A feature which has been observed for bis-tridentate Ir(III) complexes, going from the charge-neutral to the cationic forms upon methylation.¹⁹

Table 1. Selected Bond Lengths (Å) and Angles (deg) for Complexes **F1**, **F2**, **F5**, **F6**, **G3** and **G5** with Estimated Standard Deviations (es's) Given in Parentheses.

	Bond length (Å)				Bite angle (°)		$\Theta^{[a]}$
	Ir-C	Ir-N	Ir-N _{pic}	Ir-O	C _{C^N} -Ir-N _{C^N}	N _{pic} -Ir-O	
F1 ⁹	1.988(4)	2.039(3)	2.154(3)	2.149(3)	80.38(16)	76.65(13)	–
	2.007(4)	2.047(3)			80.84(16)		
F2	1.999(3)	2.034(2)	2.135(2)	2.140(18)	80.67(10)	77.51(8)	64.30(4)/ 46.20(4)
	2.006(3)	2.054(2)			80.88(10)		
F5	2.009(3)	2.048(2)	2.128(2)	2.136(2)	79.57(10)	77.70(8)	–
	2.027(3)	2.038(2)			80.21(11)		
F6	2.011(7)	2.053(6)	2.126(6)	2.138(6)	80.50(3)	77.40(2)	68.20(12) 61.40(13)
	2.033(7)	2.051(6)			80.60(3)		
	Ir-C	Ir-N _{C^N}	Ir-N _{N^N}	C-Ir-N _{C^N}	N _{N^N} -Ir-N _{N^N}	$\Theta^{[a]}$	
G3	2.014(5)	2.043(4)	2.138(4)	80.50(2)	76.54(17)	61.30(8)	
	2.019(5)	2.048(4)	2.153(4)	80.11(19)		53.00(9)	
G5	2.020(5)	2.051(5)	2.118(4)	80.40(2)	77.34(16)	–	
	2.023(5)	2.055(4)	2.131(4)	79.90(2)			

^[a] the dihedral angle between the pendant aryl ring and fluorinated ring in C^N ligands.

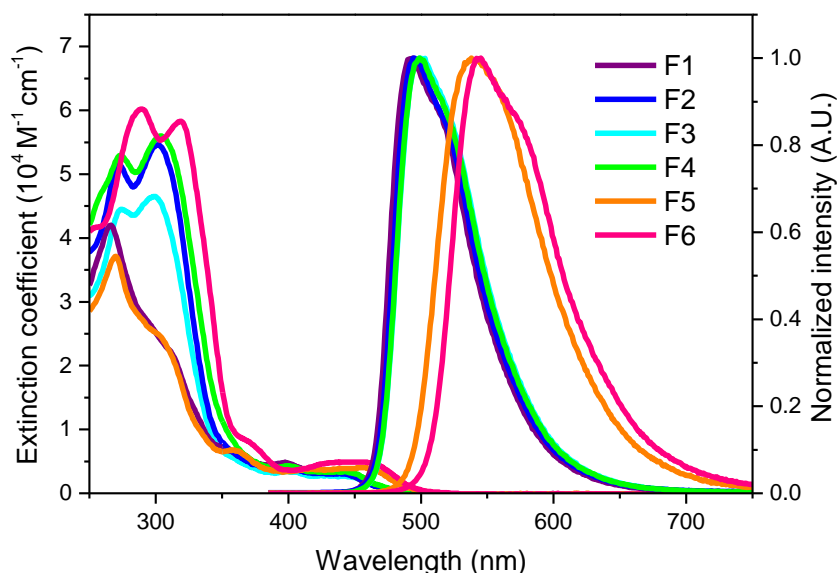


Figure 3. Absorption and emission spectra (recorded in CH₂Cl₂ at 298 K, λ_{exc} = 370 nm) of the studied charge-neutral Iridium(III) complexes **F1-F6**.

Table 2. Essential photophysical data of the studied bis-cyclometalated Ir(III) complexes **F1-F6**

	abs λ_{\max} / nm ($\epsilon / 10^4 \text{ M}^{-1} \text{ cm}^{-1}$) ^[a]	em λ_{\max} / nm ^[b]	Φ / % ^[b, c]	τ_{obs} / μs ^[b]	τ_{rad} / μs ^[b]
F1 ^[d]	266 (4.18), 312 (2.23), 398 (0.49), 443 (0.32)	492, 516 (sh)	65	1.33	2.0
F2	272 (5.16), 302 (5.45), 400 (0.41), 441 (0.31)	495, 518 (sh)	100	1.41	1.4
F3	274 (4.44), 300 (4.66), 402 (0.36), 447 (0.27)	499, 520 (sh)	100	1.48	1.5
F4	273 (5.29), 304 (5.60), 400 (0.43), 444 (0.34)	499, 519 (sh)	98	1.49	1.5
F5	270 (3.71), 307 (2.40), 359 (0.82), 461 (0.38)	537, 560 (sh)	90	3.51	3.9
F6	289 (6.02), 320 (5.84), 371 (0.82), 462 (0.51)	544, 576 (sh)	88	4.55	5.2

[a] UV-Vis spectra was recorded in CH_2Cl_2 at a conc. of 10^{-5} M at RT. [b] PL spectra, lifetime and quantum yields were recorded in degassed CH_2Cl_2 at a conc. of 10^{-5} M at RT. [c] Coumarin 153 (C153) in EtOH (Q.Y. = 58% and $\lambda_{\max} = 530$ nm) was employed as quantum yields standard. [d] our studies, for a better comparison.

Electronic absorption and emission properties. The photophysical properties of complexes **F1-F6** are summarized in Table 2, and their UV-vis. absorption and emission spectra are illustrated in Figure 3. The electronic absorption spectrum (CH_2Cl_2) of **F1** is comparable to that of the Firpic^{5e, 9} displaying an intense intraligand (IL) band in the far UV (266 nm), and a moderately intense band at lower-energy (312 nm) due to π - π^* transition of the C[^]N ligands. The weak low-energy bands at 398 and 443 nm are typically attributed to metal-to-ligand charge transfer and ligand-to-ligand charge transfer (MLCT/LLCT) transitions. The introduction of the electron-withdrawing CF_3 group on the pyridyl ring leads to a modest bathochromic shift of the lowest-energy absorption, with respect to Firpic. The profiles of the absorption bands of complexes **F2-F4** are also similar to each other, showing a broad and red-shifted intense band in the UV region (260-360 nm), due to the additional aryl group. The spectrum of **F5**, where the substitution pattern of the fluorine atoms is modified, is slightly perturbed, bathochromic shifted compared to that of **F1**. The arylated complex **F6**, shows a comparable behavior to **F2-F4**, the weaker band at wavelength longer than 400 nm has greater molar extinction coefficients, a feature also observed for the parent complex **F5**. Upon photo-excitation at $\lambda_{\text{exc}} = 370$ nm, CH_2Cl_2 solutions of the **F1-F4** complexes display intense luminescence into the blue-green region. Upon going from the unsubstituted Firpic ($\lambda_{\text{em}} = 468, 495\text{sh}$ nm)^{5e} to the 5- CF_3 -substituted derivative **F1**, the room temperature emission spectrum in dichloromethane exhibits two emission peak maxima at $\lambda = 492$ nm and 516 nm, similar in shape but red-shifted by 24 nm. The emission band of **F2** ($\Delta\lambda_{\text{em}} = 3$ nm) and those of **F3** and **F4** ($\Delta\lambda_{\text{em}} = 7$ nm) is negligible shifted when compared to the parent **F1**. As the precursor complex, their emission arises from a mixture of ³MLCT and ³LC (ligand centered) transitions, with lifetimes found in the region of 1.4 μs .^{5e} This negligible impact

observed upon arylation at the 5-position of the 4,6-difluorophenyl ring on emission arises from the almost orthogonal conformation of the appended aryl groups observed by X-ray studies and also reported in previous studies.^{10e} Notably, arylation leads to a significant enhancement of the luminescence quantum yields in dilute solution, PLQY of **F2**, **F3**, and **F4** are increased up to unity. The substituted 3,5-difluorophenylpyridinato-based complex **F6** displays an emission band peaking at 544 nm, red-shifted by 7 nm compared to that of the precursor 2-(3,5-difluorophenyl)-5-(trifluoromethyl)pyridine complex **F5**, both complexes emit in the green region with a similar quantum yield. The same bathochromic shift of 45 nm found for **F5** relative to **F1** and **F3** with respect to **F6** is attributed to the reduced impact of the electronic effect of 3,5-disubstituted fluorine atoms. The increase of luminescence lifetimes up to 4.55 μ s for **F6** suggests a more pronounced ³LC character, the quantum yields being significantly unaffected despite the observed red-shift. The improvement of QY in solution-state upon introduction of an aryl substituent in **F2–F4** is intriguing. One possible explanation for this feature could be an increase of the radiative rate constant due to a higher degree of rigidity of these congested molecules, compared to the unsubstituted complex **F1**. The bulkiness would inhibit the attainment of a coplanar conformation and lowers the extension the π -conjugation of the system since the emission wavelength and lifetimes are relatively unaffected in **F2–F4**. It may be noted that for complex **F6** having a different fluorine substitution pattern, the quantum yield does not significantly drop off despite the decrease of the emission energy, probably due to the counteracting effect of the aryl functionalization which would be expected to have a similar positive impact on ϕ as found for **F2–F4**. Moreover, our results demonstrate that the ligand modification gives rise to the enhancement of the luminescence efficiency whatever the location of the added aryl group either onto the phenyl ring or the pyridine ring of C^N ligand for the aryl-substituted pyridine ligand of FIrpic.^{10a}

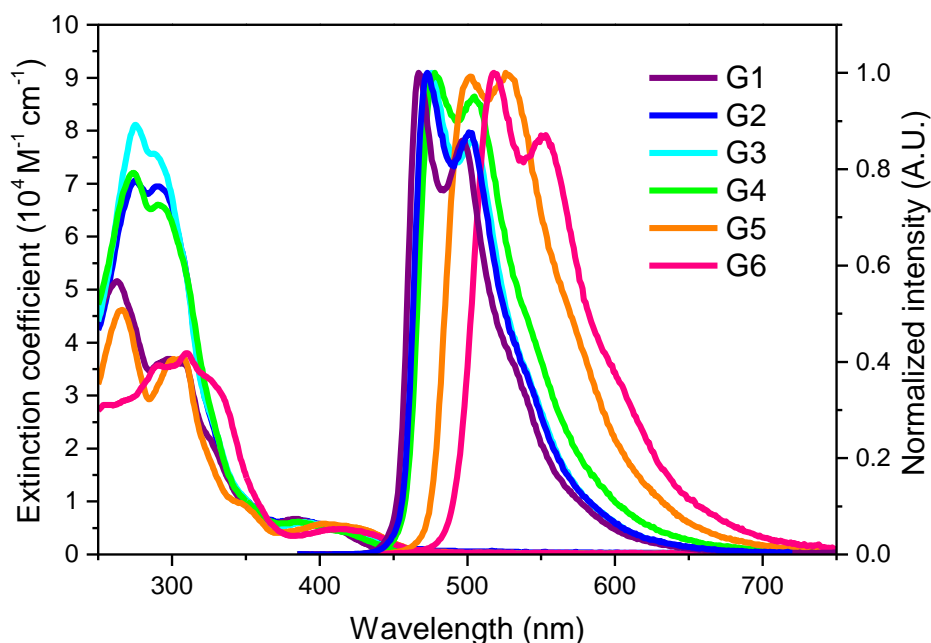


Figure 4. Absorption and emission spectra (recorded in CH_2Cl_2 at 298 K, $\lambda_{\text{exc}} = 370$ nm) of the studied charge-neutral Iridium(III) complexes **G1-G6**

Table 3. Essential photophysical data of the studied bis-cyclometalated cationic Ir(III) complexes **G1-G6**

	abs $\lambda_{\text{max}} / \text{nm}$ ($\epsilon / 10^4 \text{ M}^{-1} \text{ cm}^{-1}$) ^[a]	em $\lambda_{\text{max}} / \text{nm}$ ^[b]	$\Phi / \%$ ^[b, c]	$\tau_{\text{obs}} / \mu\text{s}$ ^[b]	$\tau_{\text{rad}} / \mu\text{s}$ ^[b]
G1	263 (5.14), 309 (3.62), 327 (2.16), 416 (0.44)	468, 497	100	2.47	2.5
G2	275 (7.07), 291 (6.95), 388 (0.66), 420 (0.47)	473, 502	83	2.69	3.2
G3	276 (8.12), 290 (7.57), 391 (0.62), 418 (0.50)	476, 504	100	2.63	2.6
G4	274 (7.20), 293 (6.59), 386 (0.60), 419 (0.42)	478, 505	100	2.42	2.4
G5	266 (4.62), 308 (3.70), 349 (0.92), 405 (0.58), 426 (0.50)	502, 527	86	4.06	4.7
G6	290 (3.57), 310 (3.80), 331 (3.12), 416 (0.50)	519, 553	70	8.39	12.0

[a] UV-Vis spectra were recorded in CH_2Cl_2 at a conc. of 10^{-5} M at RT. [b] PL spectra, lifetime and quantum yields were recorded in degassed CH_2Cl_2 at a conc. of 10^{-5} M at RT. [c] Coumarin 102 (C102) in MeOH (Q.Y. = 87% and $\lambda_{\text{max}} = 480$ nm) and Coumarin 153 (C153) in EtOH (Q.Y. = 58% and $\lambda_{\text{max}} = 530$ nm) was employed as quantum yields standard.

The second series of cationic complexes **G** dissolve in CH_2Cl_2 to give yellow orange solutions at 298 K. The electronic absorption spectra of **G1** exhibit an intense absorption band at 260–360 nm and a moderately intense band at 360–450 nm with a λ_{max} at ca. 400 nm in dichloromethane (Figure 4). The complexes **G2-G4** exhibit similar absorption spectra but with the observation of intense and very broad high-energy absorption bands from 270 nm to 380 nm due to the presence of the additional aromatic groups. As reported in the spectroscopic studies on related iridium(III) complexes,^{10e} the high-energy absorption bands

are assigned as $\pi \rightarrow \pi^*$ intraligand transitions of the C[^]N and N[^]N ligands, as well as lower-energy absorption bands in the visible region are assigned as the admixture of intraligand [$\pi \rightarrow \pi^*$] transitions and metal-to-ligand charge transfer (MLCT) [$d\pi(\text{Pt}) \rightarrow \pi^*(\text{dmbpy})$] transitions. Their electronic absorption data have been summarized in Table 3. The absorption tail (~450-500 nm) is found to show insignificant changes in the absorption profiles, these weaker absorption bands are assigned to spin-forbidden ($^3\text{MLCT}/^3\text{LC}$) transitions. As depicted in Figure 4, upon photo-excitation at $\lambda_{\text{exc}} = 370$ nm, all Ir(III) complexes show bright luminescence in fluid solution (CH_2Cl_2) at 298 K. The profiles of the emission bands are found to be insensitive to the nature of the appended aryl groups of C[^]N ligands and to the location of fluorine atoms. The complexes **G1-G4** show a small difference in emission peak wavelengths from 468 (497sh) to 478 nm (505sh). The emission ranges from blue to green, the red-shifted emission being observed for **G5** (502 nm) and **G6** (519 nm), a shift arising from the 3,5-fluorine substitution pattern, a feature also found for the related neutral complexes **F5-F6**. As expected, the different electronic effect of the fluorine in **F5-6** has an impact on the nature of the emissive excited state which gives rise to longer lifetimes (see Table 3). By comparison, note that the related complex $[\text{Ir}(\text{Phppy})_2(\text{bpy})]\text{PF}_6$, (where Phppy is 2-([1,1'-biphenyl]-3-yl)pyridine), bearing a phenyl group *trans* to the Ir-C[^]N bond exhibits a yellow-orange emission with a Φ_{PL} of 13% in CH_2Cl_2 .¹² Clearly, the combined effect of fluorine positioning in phenyl ring and a 5-CF₃-substitution of dF-ppy leads to a noteworthy improvement of PLQY values with respect to the parent complex $[\text{Ir}(\text{ppy})_2(\text{bpy})]\text{PF}_6$ (bpy = 2,2'-bipyridine). Moreover, our study shows an exceptionally high quantum yield values (unitary) for **G3** and **G4**, the steric bulk and/or electronic effect provided by the incorporated aryl group does not affect the luminescence efficiency which are similar to the parent complex **G1**. However, the positive impact, clearly seen in the **F** series, cannot be evidenced in the present case. Although **G2** displays an apparently erratic ϕ value (83%), compared to **G1** and **G3-4**, it exhibits a bright luminescence, the ϕ value being in the same range than that of its congeners. In the other hand, a slight decrease of ϕ is found for **G6**, with respect to **G5**, a trend already observed upon going from **F5** to **F6**, which could be attributed to the decrease of emission energy.

CONCLUSION

Our catalytic approach namely regioselective Pd-catalyzed C–H bond arylations applied to 2-(2,4-difluorophenyl)-5-(trifluoromethyl)pyridine (**1**) and 2-(3,5-difluorophenyl)-5-

(trifluoromethyl)pyridine (**5**) allows the access to two families of functionalized Ir(III) complexes, i.e. both the charge-neutral and cationic complexes with generalized empirical formula $[\text{Ir}(\text{C}^{\wedge}\text{N})_2(\text{N}^{\wedge}\text{O})]$ (**F**) and $[\text{Ir}(\text{C}^{\wedge}\text{N})_2(\text{N}^{\wedge}\text{N})]\text{PF}_6$ (**G**), respectively. The positions of the fluorine atoms around the cyclometalated phenyl ring are different in the two series (**F1-F4** and **G1-G4** vs. **F5, F6, G5, G6**). The incorporation of various *para*-substituted aryl appendages with an electron-withdrawing group (CN, CO₂Et, C(O)Me) occurs regioselectively at the C3- or C4-positions of the difluorobenzene ring of parent ligands **1** and **5**, respectively. X-ray crystal studies of **F2, F5, F6, G3, and G5** indicate that the intermolecular interactions are reduced, as the result of the steric bulk provided by the additional aromatic groups. The intermolecular Ir...Ir distance between adjacent complexes in crystals goes up to 15.034 Å, demonstrating the benefit of this approach in terms of bulkiness. The photophysical properties of the resulting complexes have been studied. All the investigated complexes show bright photoluminescence at room temperature in CH₂Cl₂ solution. Within the same series, the functionalized complexes display almost identical emission despite the different aryl substitution. An increase of the photoluminescence quantum yield is observed in all cases, showing the interest of such ligand design. Moreover, these functional groups (CN, CO₂Et, C(O)Me ...) might be further used as linker and grafting agents; or to modify the properties of the complexes *e.g.*, hydrophilicity, lipophilicity, key features in the fabrication of devices. This work represents a convenient route for the addition of functional and bulky groups to cyclometalated Ir(III) complexes, potentially useful for applications in opto-electronics. Studies on other metal systems are currently under way.

EXPERIMENTAL SECTION

General Information. All reactions were carried out under argon atmosphere with standard Schlenk techniques. DMA and ethoxyethanol were purchased from Acros Organics and were not purified before use. ¹H, ¹³C and ¹⁹F NMR spectra were recorded on Bruker AV III 400 MHz NMR spectrometer equipped with BBFO probehead. Chemical shifts (δ) were reported in parts per million relative to residual chloroform (7.28 ppm for ¹H; 77.23 ppm for ¹³C), constants were reported in Hertz. ¹H NMR assignment abbreviations were the following: singlet (s), doublet (d), triplet (t), quartet (q), doublet of doublets (dd), doublet of triplets (dt), and multiplet (m). All reagents were weighed and handled in air. HRMS were recorded on a Bruker Ultraflex III mass spectrometer at the corresponding facilities of the Centre Régional de Mesures Physiques de l'Ouest, Université de Rennes 1 (CRMPO). Elemental Analysis

were recorded on a Thermo Fisher FLASH 1112 at the corresponding facilities of the CRMPO. UV-Vis spectra were recorded on a HITACHI U-3900 spectrophotometer. The steady-state emission spectra and lifetime studies were measured with Edinburgh FL 900 photon-counting system. Both wavelength-dependent excitation and emission responses of the fluorimeter were calibrated. Spectral grade solvents (Merck) were used as received. To determine the photoluminescence quantum yield in solution, samples were degassed using at least three freeze-pump-thaw cycles. The solution quantum yields are calculated using the standard sample which has a known quantum yield. Cyclic voltammetry was conducted on a CHI621A Electrochemical Analyzer. Ag/Ag⁺ (0.01 M AgNO₃) electrode was employed as reference electrode. The oxidation and reduction potentials were measured using a platinum working electrode with 0.1 M of NBu₄PF₆ in CH₂Cl₂ and a gold wire with 0.1 M of NBu₄PF₆ in THF, respectively. The potentials were referenced externally to the ferrocenium/ferrocene (Fc⁺/Fc) couple.

Preparation of the PdCl(dppb)(C₃H₅) catalyst²⁰: An oven-dried 40-mL Schlenk tube equipped with a magnetic stirring bar under argon atmosphere, was charged with [Pd(C₃H₅)Cl]₂ (182 mg, 0.5 mmol) and dppb (426 mg, 1 mmol). 10 mL of anhydrous dichloromethane were added, then the solution was stirred at room temperature for twenty minutes. The solvent was removed in vacuum. The yellow powder was used without purification. ³¹P NMR (81 MHz, CDCl₃) δ (ppm) = 19.3 (s).

2-(2,4-Difluorophenyl)-5-(trifluoromethyl)pyridine (1): To a 15 mL oven dried Schlenk tube, 2-chloro-5-(trifluoromethyl)pyridine (1.81 g 10 mmol), (2,4-difluorophenyl)boronic acid (1.97 g, 12.5 mmol), K₂CO₃ (2.76 g, 20 mmol), toluene (16 mL), MeOH (2 mL) water (2 mL) and PdCl(C₃H₅)(dppb) (0.120 g, 0.2 mmol, 2 mol%) were successively added. The reaction mixture was evacuated by vacuum-argon cycles (5 times) and stirred at 110 °C (oil bath temperature) for 16 hours. After cooling the reaction at room temperature and concentration, the crude mixture was purified by flash chromatography on silica gel (EtOAc-Heptane, 80:20) to afford the desired compound **1** (2.12 g, 82%). The NMR data were consistent with those reported in the literature.²¹

2',6'-Difluoro-3'-(5-(trifluoromethyl)pyridin-2-yl)-[1,1'-biphenyl]-4-carbonitrile (2): To a 15 mL oven dried Schlenk tube, 2-(2,4-difluorophenyl)-5-(trifluoromethyl)pyridine (**1**) (259

mg, 1.00 mmol), 4-bromobenzonitrile (273 mg, 1.5 mmol), PivOK (280 mg, 2 mmol), DMA (3 mL) and PdCl(C₃H₅)(dppb) (30 mg, 0.05 mmol, 5 mol%) were successively added. The reaction mixture was evacuated by vacuum-argon cycles (5 times) and stirred at 150 °C (oil bath temperature) for 48 hours. After cooling the reaction at room temperature and concentration, the crude mixture was purified by flash chromatography on silica gel (EtOAc-Heptane, 80:20) to afford the desired compound **2** (230 mg, 64%). ¹H NMR (400 MHz, CDCl₃) δ (ppm) 9.02 (d, *J* = 2.3 Hz, 1H), 8.14 (td, *J* = 6.4, 8.8 Hz, 1H), 8.04 (dd, *J* = 2.4, 8.4 Hz, 1H), 7.93 (dd, *J* = 2.2, 8.3 Hz, 1H), 7.81 (d, *J* = 8.0 Hz, 2H), 7.66 (d, *J* = 8.0 Hz, 2H), 7.22 (t, *J* = 8.8 Hz, 1H). ¹⁹F{¹H} NMR (376 MHz, CDCl₃) δ (ppm) -62.4 (s), -111.0 (d, *J* = 9.4 Hz), -116.8 (d, *J* = 9.4 Hz). ¹³C{¹H} NMR (100 MHz, CDCl₃) δ (ppm) 160.5 (dd, *J* = 6.4, 253.8 Hz), 157.5 (dd, *J* = 6.6, 254.4 Hz), 155.6, 146.6 (q, *J* = 3.9 Hz), 133.8 (q, *J* = 3.3 Hz), 133.7, 132.0, 131.2, 125.4 (q, *J* = 33.2 Hz), 123.8 (d, *J* = 10.7 Hz), 123.5 (q, *J* = 271.4 Hz), 123.1 (dd, *J* = 3.8, 12.6 Hz), 118.5, 117.3 (t, *J* = 19.1 Hz), 112.6 (dd, *J* = 3.7, 22.8 Hz), 112.4. Elemental analysis: calcd (%) for C₁₉H₉F₅N₂ (360.29): C 63.34, H 2.52, N 7.78; found: C 63.09, H 2.65, N 7.98.

Ethyl 2',6'-difluoro-3'-(5-(trifluoromethyl)pyridin-2-yl)-[1,1'-biphenyl]-4-carboxylate (3): To a 15 mL oven dried Schlenk tube, 2-(2,4-difluorophenyl)-5-(trifluoromethyl)pyridine (**1**) (259 mg, 1.00 mmol), ethyl 4-bromobenzoate (343 mg, 1.5 mmol), PivOK (280 mg, 2 mmol), DMA (3 mL) and PdCl(C₃H₅)(dppb) (30 mg, 0.05 mmol, 5 mol%) were successively added. The reaction mixture was evacuated by vacuum-argon cycles (5 times) and stirred at 150 °C (oil bath temperature) for 48 hours. After cooling the reaction at room temperature and concentration, the crude mixture was purified by flash chromatography on silica gel (EtOAc-Heptane, 70:30) to afford the desired compound **3** (277 mg, 68%). ¹H NMR (400 MHz, CDCl₃) δ (ppm) 9.00 (d, *J* = 2.3 Hz, 1H), 8.19 (d, *J* = 8.0 Hz, 2H), 8.11 (td, *J* = 6.4, 8.7 Hz, 1H), 8.01 (dd, *J* = 2.4, 8.4 Hz, 1H), 7.93 (dd, *J* = 2.1, 8.4 Hz, 1H), 7.60 (d, *J* = 8.0 Hz, 2H), 7.19 (t, *J* = 8.7 Hz, 1H), 4.44 (q, *J* = 7.1 Hz, 2H), 1.44 (t, *J* = 7.1 Hz, 3H). ¹⁹F{¹H} NMR (376 MHz, CDCl₃) δ (ppm) -62.4 (s), -110.8 (d, *J* = 8.0 Hz), -116.6 (d, *J* = 8.0 Hz). ¹³C{¹H} NMR (100 MHz, CDCl₃) δ (ppm) 166.2, 160.7 (dd, *J* = 6.7, 253.4 Hz), 157.7 (dd, *J* = 6.9, 253.9 Hz), 155.8, 146.6 (q, *J* = 4.0 Hz), 133.8 (q, *J* = 3.6 Hz), 133.4, 131.4 (dd, *J* = 4.4, 10.3 Hz), 130.5, 130.4, 129.5, 125.3 (q, *J* = 33.2 Hz), 123.8 (d, *J* = 10.8 Hz), 123.5 (q, *J* = 271.4 Hz), 123.0 (dd, *J* = 3.9, 12.7 Hz), 118.2 (t, *J* = 19.6 Hz), 112.5 (dd, *J* = 3.8, 22.8 Hz), 61.1,

14.3. Elemental analysis: calcd (%) for C₂₁H₁₄F₅NO₂ (407.34): C 61.92, H 3.46, N 3.44; found: C 62.08, H 3.59, N 3.21.

1-(2',6'-Difluoro-3'-(5-(trifluoromethyl)pyridin-2-yl)-[1,1'-biphenyl]-4-yl)ethan-1-one

(4): To a 15 mL oven dried Schlenk tube, 2-(2,4-difluorophenyl)-5-(trifluoromethyl)pyridine (**1**) (259 mg, 1.00 mmol), 4-bromoacetophenone (299 mg, 1.5 mmol), PivOK (280 mg, 2 mmol), DMA (3 mL) and PdCl(C₃H₅)(dppb) (30 mg, 0.05 mmol, 5 mol%) were successively added. The reaction mixture was evacuated by vacuum-argon cycles (5 times) and stirred at 150 °C (oil bath temperature) for 48 hours. After cooling the reaction at room temperature and concentration, the crude mixture was purified by flash chromatography on silica gel (EtOAc-Heptane, 70:30) to afford the desired compound **4** (230 mg, 61%). ¹H NMR (400 MHz, CDCl₃) δ (ppm) 9.01 (s, 1H), 8.17 – 8.06 (m, 3H), 8.02 (dd, *J* = 2.3, 8.4 Hz, 1H), 7.93 (d, *J* = 8.3 Hz, 1H), 7.64 (d, *J* = 7.9 Hz, 2H), 7.20 (t, *J* = 8.7 Hz, 1H), 2.68 (s, 3H). ¹⁹F{¹H} NMR (376 MHz, CDCl₃) δ (ppm) -62.4, -110.8 (d, *J* = 8.0 Hz), -116.6 (d, *J* = 8.0 Hz). ¹³C{¹H} NMR (100 MHz, CDCl₃) δ (ppm) 197.6, 160.7 (dd, *J* = 6.7, 253.5 Hz), 157.7 (dd, *J* = 6.9, 254.0 Hz), 155.8, 146.6 (q, *J* = 4.0 Hz), 136.9, 133.8 (q, *J* = 3.5 Hz), 133.7, 131.5 (dd, *J* = 4.4, 10.3 Hz), 130.7, 128.3, 125.3 (q, *J* = 33.2 Hz), 123.8 (d, *J* = 10.7 Hz), 123.5 (q, *J* = 271.8 Hz), 123.0 (dd, *J* = 4.0, 12.7 Hz), 118.0 (t, *J* = 19.6 Hz), 112.5 (dd, *J* = 3.8, 22.8 Hz), 26.7. Elemental analysis: calcd (%) for C₂₀H₁₂F₅NO (277.31): C 63.67, H 3.21, N 3.71; found: C 64.01, H 3.19, N 3.56.

2-(3,5-Difluorophenyl)-5-(trifluoromethyl)pyridine (5): To a 15 mL oven dried Schlenk tube, 2-chloro-5-(trifluoromethyl)pyridine (1.81 g 10 mmol), (3,5-difluorophenyl)boronic acid (1.97 g, 12.5 mmol), K₂CO₃ (2.76 g, 20 mmol), toluene (16 mL), MeOH (2 mL) water (2 mL) and PdCl(C₃H₅)(dppb) (0.120 g, 0.2 mmol, 2 mol%) were successively added. The reaction mixture was evacuated by vacuum-argon cycles (5 times) and stirred at 110 °C (oil bath temperature) for 16 hours. After cooling the reaction at room temperature and concentration, the crude mixture was purified by flash chromatography on silica gel (EtOAc-Heptane, 80:20) to afford the desired compound **5** (2.07 g, 80%). ¹H NMR (400 MHz, CDCl₃) δ (ppm) 8.96 (s, 1H), 8.03 (d, *J* = 8.3 Hz, 1H), 7.81 (d, *J* = 8.3 Hz, 1H), 7.60 (d, *J* = 7.2 Hz, 2H), 6.93 (t, *J* = 8.7 Hz, 1H). ¹⁹F{¹H} NMR (376 MHz, CDCl₃) δ (ppm) -62.5 (S), -108.8 (S). ¹³C{¹H} NMR (100 MHz, CDCl₃) δ (ppm) 163.4 (dd, *J* = 12.7, 248.6 Hz), 157.7,

146.7 (q, $J = 4.1$ Hz), 141.0 (t, $J = 9.4$ Hz), 134.2 (q, $J = 3.5$ Hz), 125.9 (q, $J = 33.3$ Hz), 123.5 (q, $J = 272.3$ Hz), 119.8, 110.1 (d, $J = 26.7$ Hz), 105.2 (t, $J = 25.5$ Hz). Elemental analysis: calcd (%) for $C_{12}H_6F_5N$ (259.18): C 55.61, H 2.33, N 5.40; found: C 55.68, H 2.49, N 5.68.

Ethyl 3',5'-difluoro-3'-(5-(trifluoromethyl)pyridin-2-yl)-[1,1'-biphenyl]-4-carboxylate (6): To a 15 mL oven dried Schlenk tube, 2-(3,5-difluorophenyl)-5-(trifluoromethyl)pyridine (**5**) (259 mg, 1.00 mmol), ethyl 4-bromobenzoate (343 mg, 1.5 mmol), PivOK (280 mg, 2 mmol), DMA (3 mL) and $PdCl_2(C_3H_5)_2(dppb)$ (30 mg, 0.05 mmol, 5 mol%) were successively added. The reaction mixture was evacuated by vacuum-argon cycles (5 times) and stirred at 150 °C (oil bath temperature) for 48 hours. After cooling the reaction at room temperature and concentration, the crude mixture was purified by flash chromatography on silica gel (EtOAc-Heptane, 70:30) to afford the desired compound **6** (293 mg, 72%). 1H NMR (400 MHz, $CDCl_3$) δ (ppm) 8.97 (s, 1H), 8.16 (d, $J = 8.0$ Hz, 2H), 8.03 (d, $J = 8.4$ Hz, 1H), 7.85 (d, $J = 8.3$ Hz, 1H), 7.75 (d, $J = 8.4$ Hz, 2H), 7.61 (d, $J = 8.0$ Hz, 2H), 4.43 (q, $J = 7.2$ Hz, 2H), 1.43 (t, $J = 7.1$ Hz, 3H). $^{19}F\{^1H\}$ NMR (376 MHz, $CDCl_3$) δ (ppm) -62.4 (s), -112.9 (s). $^{13}C\{^1H\}$ NMR (100 MHz, $CDCl_3$) δ (ppm) 166.1, 160.3 (dd, $J = 7.4, 249.7$ Hz), 157.4, 146.8 (q, $J = 4.0$ Hz), 139.6 (t, $J = 9.8$ Hz), 134.3 (q, $J = 3.5$ Hz), 133.2, 130.5, 130.3, 129.5, 125.9 (q, $J = 33.2$ Hz), 123.5 (q, $J = 271.5$ Hz), 119.8, 118.9 (t, $J = 18.6$ Hz), 110.5 (d, $J = 27.9$ Hz), 61.1, 14.3. Elemental analysis: calcd (%) for $C_{21}H_{14}F_5NO_2$ (407.34): C 61.92, H 3.46, N 3.44; found: C 62.12, H 3.23, N 3.56.

Iridium(III) bis[2-(2,4-difluorophenyl)-5-(trifluoromethyl)pyridinato-N,C^{2'}]picolinate (F1): $IrCl_3 \cdot 6H_2O$ (75 mg, 0.25 mmol, 1.0 eq.) and 2-(2,4-difluorophenyl)-5-(trifluoromethyl)pyridine (**1**) (142 mg, 0.55 mmol, 2.2 eq.) were suspended in a mixture of 2-ethoxyethanol/water (5 mL, 3/1). The mixture was heated and kept at 125 °C under stirring. After 24 h, it was allowed to cool to room temperature and the solvent was removed under vacuo to give the intermediate $[Ir(C^{\wedge}N)_2Cl]_2$ dimer complex, which was directly engaged in the next step without further purification. This complex and picolinic acid (104 mg, 0.75 mmol, 6 eq.) were dissolved in 2-ethoxyethanol (8 mL), and Na_2CO_3 (159 mg, 1.5 mmol, 6 eq.) was added. The solution was heated at 125 °C for 24 h. The solution was allowed to cool to room temperature. After concentration, the residue was purified by flash chromatography

on silica gel (CH₂Cl₂- EtOAc, 75:25) to afford the desired complex **F1** (135 mg, 65%). ¹H NMR (400 MHz, CDCl₃) δ (ppm) 9.02 (s, 1H), 8.47 – 8.36 (m, 3H), 8.12 – 7.96 (m, 3H), 7.79 (d, *J* = 5.3 Hz, 1H), 7.54 (t, *J* = 6.6 Hz, 1H), 7.50 (s, 1H), 6.56 (t, *J* = 10.7 Hz, 1H), 6.46 (t, *J* = 10.8 Hz, 1H), 5.82 (d, *J* = 8.3 Hz, 1H), 5.55 (d, *J* = 8.4 Hz, 1H). ¹⁹F{¹H} NMR (376 MHz, CDCl₃) δ (ppm) -62.1, -62.8, -103.4 (d, *J* = 12.3 Hz), -104.3 (d, *J* = 11.7 Hz), -107.30(d, *J* = 11.9 Hz), -108.1 (d, *J* = 11.6 Hz). ¹³C{¹H} NMR (100 MHz, CDCl₃) δ (ppm) 172.1, 169.1 (d, *J* = 7.0 Hz), 167.7 (d, *J* = 6.9 Hz), 164.5 (dd, *J* = 12.9, 260.0 Hz), 164.1 (dd, *J* = 12.6, 259.3 Hz), 162.4 (dd, *J* = 10.5, 261.9 Hz), 162.2 (dd, *J* = 10.2, 262.0 Hz), 153.5 (d, *J* = 7.2 Hz), 152.4 (d, *J* = 7.3 Hz), 151.4, 148.3, 145.6 (q, *J* = 4.3 Hz), 144.5 (q, *J* = 4.8 Hz), 139.2, 135.8 – 135.5 (m), 129.0 (d, *J* = 3.6 Hz), 126.9 – 126.7 (m), 125.5 (q, *J* = 34.9 Hz), 125.1 (q, *J* = 34.7 Hz), 123.0 (d, *J* = 21.1 Hz), 122.5 (d, *J* = 19.9 Hz), 122.1 (q, *J* = 271.4 Hz), 121.9 (q, *J* = 270.4 Hz), 114.9 (dd, *J* = 2.7, 17.4 Hz), 114.6 (dd, *J* = 2.7, 17.7 Hz), 98.9 (d, *J* = 27.3 Hz), 98.4 (d, *J* = 27.1 Hz). MALDI HRMS for C₃₀H₁₅N₃F₁₀¹⁹³Ir [M+H]⁺: found 832.0062, calcd 832.066. Elemental analysis: calcd (%) for C₃₀H₁₄N₃F₁₀Ir (831.05): C 43.38, H 1.70, N 5.06; found: C 43.24, H 1.45, N 5.02

Iridium(III) bis[2-(4'-cyano-2,6-difluoro-[1,1'-biphenyl]-3-yl)-5-(trifluoromethyl)pyridinato-N,C^{2'}]picolinate (F2): IrCl₃·6H₂O (75 mg, 0.25 mmol, 1.0 eq.) and 2',6'-difluoro-3'-(5-(trifluoromethyl)pyridin-2-yl)-[1,1'-biphenyl]-4-carbonitrile (**2**) (198 mg, 0.55 mmol, 2.2 eq.) were suspended in a mixture of 2-ethoxyethanol/water (5 mL, 3/1). The mixture was heated and kept at 125 °C under stirring. After 24 h, it was allowed to cool to room temperature and the solvent was removed under vacuo to give the intermediate [Ir(C^N)₂Cl]₂ dimer complex, which was directly engaged in the next step without further purification. This complex and picolinic acid (104 mg, 0.75 mmol, 6 eq.) were dissolved in 2-ethoxyethanol (8 mL), and Na₂CO₃ (159 mg, 1.5 mmol, 6 eq.) was added. The solution was heated at 125 °C for 24 h. The solution was allowed to cool to room temperature. After concentration, the residue was purified by flash chromatography on silica gel (CH₂Cl₂-EtOAc, 75:25) to afford the desired complex **F2** (176 mg, 68%). ¹H NMR (400 MHz, CDCl₃) δ (ppm) 9.09 (s, 1H), 8.53 – 8.42 (m, 3H), 8.16 – 8.07 (m, 3H), 7.92 (d, *J* = 5.3 Hz, 1H), 7.81 – 7.69 (m, 3H), 7.68 – 7.57 (m, 4H), 7.56 – 7.46 (m, 3H), 6.06 (d, *J* = 9.2 Hz, 1H), 5.75 (d, *J* = 9.2 Hz, 1H). ¹⁹F{¹H} NMR (376 MHz, CDCl₃) δ (ppm) -62.1 (s), -62.8 (s), -107.6 (d, *J* = 11.1 Hz), -108.4 (d, *J* = 10.9 Hz), -112.5 (d, *J* = 11.1 Hz), -113.2 (d, *J* = 11.1

Hz). $^{13}\text{C}\{^1\text{H}\}$ NMR (100 MHz, CDCl_3) δ (ppm) 172.0, 168.9 (d, $J = 6.9$ Hz), 167.7, 167.6 (d, $J = 7.2$ Hz), 160.9 (dd, $J = 7.0, 261.6$ Hz), 160.5 (dd, $J = 6.8, 260.9$ Hz), 158.6 (dd, $J = 7.6, 263.5$ Hz), 158.5 (dd, $J = 7.4, 262.7$ Hz), 153.3 (d, $J = 7.6$ Hz), 152.5 (d, $J = 7.7$ Hz), 151.3, 148.4, 145.8 (q, $J = 4.3$ Hz), 144.7 (q, $J = 4.5$ Hz), 139.6, 136.1, 134.3 (d, $J = 22.9$ Hz), 132.3, 132.0 (d, $J = 7.3$ Hz), 131.0 (d, $J = 4.6$ Hz), 130.9, 129.2 (d, $J = 11.7$ Hz), 128.8, 127.6 – 127.4 (m), 126.1 (q, $J = 35.6$ Hz), 125.7 (q, $J = 36.0$ Hz), 123.4 (d, $J = 22.9$ Hz), 122.9 (d, $J = 21.3$ Hz), 121.9 (q, $J = 271.4$ Hz), 121.8 (q, $J = 271.4$ Hz), 118.6 (d, $J = 9.3$ Hz), 115.6 (d, $J = 18.7$ Hz), 115.2 (d, $J = 19.3$ Hz), 111.8, 111.7, 111.5 (t, $J = 19.7$ Hz), 111.0 (t, $J = 19.3$ Hz). MALDI HRMS for $\text{C}_{44}\text{H}_{21}\text{N}_5\text{O}_2\text{F}_{10}^{193}\text{Ir}$ $[\text{M}+\text{H}]^+$: found 1034.1160, calcd 1034.121. Elemental analysis: calcd (%) for $\text{C}_{44}\text{H}_{20}\text{N}_5\text{O}_2\text{F}_{10}\text{Ir}$ (1032.87): C 51.17, H 1.95, N 6.78; found: C 51.08, H 2.12, N 6.98

Iridium(III) bis[2-((4'-(ethoxycarbonyl)-2,6-difluoro-[1,1'-biphenyl] 3-yl)-5-(trifluoromethyl)pyridinato-N,C^{2'})picolinate (F3): $\text{IrCl}_3 \cdot 6\text{H}_2\text{O}$ (75 mg, 0.25 mmol, 1.0 eq.) and ethyl 2',6'-difluoro-3'-(5-(trifluoromethyl)pyridin-2-yl)-[1,1'-biphenyl]-4-carboxylate (**3**) (224 mg, 0.55 mmol, 2.2 eq.) were suspended in a mixture of 2-ethoxyethanol/water (5 mL, 3/1). The mixture was heated and kept at 125 °C under stirring. After 24 h, it was allowed to cool to room temperature and the solvent was removed under vacuo to give the dimer $[\text{Ir}(\text{C}^{\wedge}\text{N})_2\text{Cl}]_2$, which was directly engaged in the next step without further purification. This complex and picolinic acid (104 mg, 0.75 mmol, 6 eq.) were dissolved in 2-ethoxyethanol (8 mL), and Na_2CO_3 (159 mg, 1.5 mmol, 6 eq.) was added. The solution was heated at 125 °C for 24 h. The solution was allowed to cool to room temperature. After concentration, the residue was purified by flash chromatography on silica gel (CH_2Cl_2 - EtOAc, 75:25) to afford the desired complex **F3** (175 mg, 62%). ^1H NMR (400 MHz, Acetone- d_6) δ (ppm) 9.13 (s, 1H), 8.63 (t, $J = 7.3$ Hz, 2H), 8.44 (t, $J = 9.4$ Hz, 2H), 8.32 – 8.22 (m, 2H), 8.16 (d, $J = 5.3$ Hz, 1H), 8.14 – 8.08 (m, 4H), 7.90 (s, 1H), 7.78 – 7.71 (m, 1H), 7.68 – 7.60 (m, 4H), 6.29 (d, $J = 9.6$ Hz, 1H), 5.94 (d, $J = 9.5$ Hz, 1H), 4.40 (q, $J = 7.3, 8.3$ Hz, 2H), 4.39 (q, $J = 7.3, 8.3$ Hz, 2H), 1.40 (t, $J = 7.1$ Hz, 3H), 1.39 (t, $J = 7.1$ Hz, 3H). $^{19}\text{F}\{^1\text{H}\}$ NMR (376 MHz, Acetone- d_6) δ (ppm) -63.2 (d, $J = 154.6$ Hz), -110.0 (d, $J = 12.1$ Hz), -110.6 (d, $J = 11.9$ Hz), -113.7 (d, $J = 12.1$ Hz), -114.1 (d, $J = 12.0$ Hz). $^{13}\text{C}\{^1\text{H}\}$ NMR (100 MHz, Acetone- d_6) δ (ppm) 172.0, 168.6 (d, $J = 7.1$ Hz), 168.0 (d, $J = 7.2$ Hz), 165.6, 161.0 (dd, $J = 7.4, 258.5$ Hz), 160.5 (dd, $J = 7.4, 257.9$ Hz), 158.9 (dd, $J = 7.4, 261.8$ Hz), 158.5 (dd, $J = 7.4, 261.9$

Hz), 154.5 (d, $J = 7.6$ Hz), 152.7 (d, $J = 7.8$ Hz), 151.4, 149.4, 145.5 (q, $J = 4.5$ Hz), 145.2 (q, $J = 4.1$ Hz), 139.8, 136.7, 134.4, 130.5, 130.5 (m), 130.0, 129.4, 129.1 (m), 128.3, 127.7 (m), 125.3 (d, $J = 16.7$ Hz), 124.9 (d, $J = 16.2$ Hz), 124.0 – 123.2 (m), 121.2 (d, $J = 23.9$ Hz), 115.7 (d, $J = 19.3$ Hz), 114.8 (d, $J = 18.7$ Hz), 112.0 – 111.1 (m), 60.7, 13.7. MALDI HRMS for $C_{48}H_{31}N_3O_6F_{10}^{193}Ir [M+H]^+$: found 1128.1677, calcd 1128.170. Elemental analysis: calcd (%) for $C_{48}H_{30}N_3O_6F_{10}Ir$ (1126.28): C 51.16, H 2.68, N 3.73; found: C 51.21, H 2.89, N 3.23.

Iridium(III)

bis[2-(4'-acetyl-2,6-difluoro-[1,1'-biphenyl]-3-yl)-5-

(trifluoromethyl)pyridinato-N,C^{2'}]picolinate (**F4**): $IrCl_3 \cdot 6H_2O$ (75 mg, 0.25 mmol, 1.0 eq.) and 1-(2',6'-difluoro-3'-(5-(trifluoromethyl)pyridin-2-yl)-[1,1'-biphenyl]-4-yl)ethan-1-one (**4**) (153 mg, 0.55 mmol, 2.2 eq.) were suspended in a mixture of 2-ethoxyethanol/water (5 mL, 3/1). The mixture was heated and kept at 125 °C under stirring. After 24 h, it was allowed to cool to room temperature and the solvent was removed under vacuo to give the intermediate $[Ir(C^{\wedge}N)_2Cl]_2$ dimer complex, which was directly engaged in the next step without further purification. This complex and picolinic acid (104 mg, 0.75 mmol, 6 eq.) were dissolved in 2-ethoxyethanol (8 mL), and Na_2CO_3 (159 mg, 1.5 mmol, 6 eq.) was added. The solution was heated at 125 °C for 24 h. The solution was allowed to cool to room temperature. After concentration, the residue was purified by flash chromatography on silica gel (CH_2Cl_2 -EtOAc, 75:25) to afford the desired complex **F4** (160 mg, 60%). 1H NMR (400 MHz, $CDCl_3$) δ (ppm) 9.10 (s, 1H), 8.55 – 8.34 (m, 3H), 8.12 – 7.94 (m, 7H), 7.94 (s, 1H), 7.65 – 7.54 (m, 4H), 7.50 (d, $J = 8.0$ Hz, 2H), 6.06 (d, $J = 9.2$ Hz, 1H), 5.75 (d, $J = 9.2$ Hz, 1H), 2.65 (s, 3H), 2.63 (s, 3H). $^{19}F\{^1H\}$ NMR (376 MHz, $CDCl_3$) δ (ppm) -62.2 (s), -62.8 (s), -107.2 (d, $J = 11.4$ Hz), -108.1 (d, $J = 11.3$ Hz), -112.2 (d, $J = 11.7$ Hz), -112.9 (d, $J = 11.7$ Hz). $^{13}C\{^1H\}$ NMR (100 MHz, $CDCl_3$) δ (ppm) 197.6, 197.5, 172.0, 169.1 (d, $J = 7.0$ Hz), 167.8 (d, $J = 6.7$ Hz), 161.2 (dd, $J = 7.1, 261.3$ Hz), 160.8 (dd, $J = 6.7, 260.6$ Hz), 158.9 (dd, $J = 10.0, 264.9$ Hz), 158.8 (dd, $J = 7.5, 262.6$ Hz), 152.6 (d, $J = 7.6$ Hz), 151.7 (d, $J = 7.4$ Hz), 151.4, 148.4, 145.8 (q, $J = 4.6$ Hz), 144.7 (q, $J = 4.9$ Hz), 139.4, 136.4 (d, $J = 10.8$ Hz), 135.9, 134.3 (d, $J = 25.8$ Hz), 130.5, 129.1 (d, $J = 10.9$ Hz), 128.2 (d, $J = 7.2$ Hz), 127.4 (m), 125.9 (q, $J = 36.7$ Hz), 125.5 (d, $J = 35.8$ Hz), 123.3 (d, $J = 3.9$ Hz), 122.8 (d, $J = 21.3$ Hz), 122.0 (q, $J = 272.1$ Hz), 121.9 (q, $J = 272.1$ Hz), 115.5 (d, $J = 18.9$ Hz), 115.1 (d, $J = 19.1$ Hz), 112.2 (t, $J = 19.9$ Hz), 111.7 (t, $J = 19.7$ Hz), 26.6. MALDI HRMS for

$C_{46}H_{27}N_3O_4F_{10}^{193}Ir$ [M+H]⁺: found 1068.1466, calcd 1068.145. Elemental analysis: calcd (%) for $C_{46}H_{26}N_3O_4F_{10}Ir$ (1066.93): C 51.78, H 2.46, N 3.94 found: C 51.88, H 2.43, N 4.12.

Iridium(III) bis[2-(3,5-difluorophenyl)-5-(trifluoromethyl)pyridinato-N,C^{2'}]picolinate (F5): $IrCl_3 \cdot 6H_2O$ (75 mg, 0.25 mmol, 1.0 eq.) and 2-(3,5-difluorophenyl)-5-(trifluoromethyl)pyridine (**5**) (142 mg, 0.55 mmol, 2.2 eq.) were suspended in a mixture of 2-ethoxyethanol/water (5 mL, 3/1). The mixture was heated and kept at 125 °C under stirring. After 24 h, it was allowed to cool to room temperature and the solvent was removed under vacuo to give the intermediate $[Ir(C^N)_2Cl]_2$ dimer complex, which was directly engaged in the next step without further purification. This complex and picolinic acid (104 mg, 0.75 mmol, 6 eq.) were dissolved in 2-ethoxyethanol (8 mL), and Na_2CO_3 (159 mg, 1.5 mmol, 6 eq.) was added. The solution was heated at 125 °C for 24 h. The solution was allowed to cool to room temperature. After concentration, the residue was purified by flash chromatography on silica gel (CH_2Cl_2 - EtOAc, 75:25) to afford the desired complex **F5** (141 mg, 68%). ¹H NMR (400 MHz, Acetone-*d*₆) δ (ppm) 9.09 (s, 1H), 8.49 (t, *J* = 7.8 Hz, 2H), 8.32 (d, *J* = 8.6 Hz, 2H), 8.28 – 8.19 (m, 2H), 8.00 (d, *J* = 5.3 Hz, 1H), 7.83 (dd, *J* = 2.5, 9.4 Hz, 1H), 7.79 – 7.66 (m, 3H), 6.60 (td, *J* = 2.4, 9.3 Hz, 1H), 6.49 (td, *J* = 2.4, 9.5 Hz, 1H). ¹⁹F{¹H} NMR (376 MHz, Acetone-*d*₆) δ (ppm) -63.0, -63.5, -102.2 (d, *J* = 5.8 Hz), -103.9 (d, *J* = 5.8 Hz), -120.6 (d, *J* = 6.0 Hz), -120.7 (d, *J* = 5.8 Hz). ¹³C{¹H} NMR (100 MHz, Acetone-*d*₆) δ (ppm) 171.8, 171.4 (d, *J* = 4.3 Hz), 170.9 (d, *J* = 3.0 Hz), 169.1 (dd, *J* = 11.2, 238.3 Hz), 168.8 (dd, *J* = 11.2, 245.1 Hz), 159.9 (dd, *J* = 12.5, 238.7 Hz), 159.7 (dd, *J* = 12.1, 238.5 Hz), 151.6, 149.2, 147.4 – 146.8 (m), 145.8 – 145.2 (m), 139.7, 135.7 – 135.5 (m), 129.5, 128.4, 125.1 (d, *J* = 8.9 Hz), 124.8 (d, *J* = 9.1 Hz), 127.9, 124.1 (q, *J* = 272.1 Hz), 122.5 (q, *J* = 271.8 Hz), 122.4, 122.1, 120.6, 120.3, 109.1 (dd, *J* = 3.8, 22.2 Hz), 108.7 (dd, *J* = 3.8, 22.0 Hz), 105.6 (dd, *J* = 24.9, 62.0 Hz), 105.6 (dd, *J* = 2.2, 24.8 Hz). MALDI HRMS for $C_{30}H_{15}N_3F_{10}^{193}Ir$ [M+H]⁺: found 832.0062, calcd 832.066. Elemental analysis: calcd (%) for $C_{30}H_{14}N_3F_{10}Ir$ (831.05): C 43.38, H 1.70, N 5.06; found: C 43.65, H 1.67, N 5.26

Iridium(III) bis[2-((4'-(ethoxycarbonyl)-3,5-difluoro-[1,1'-biphenyl]-4-yl)-5-(trifluoromethyl)pyridinato-N,C^{2'}]picolinate (F6): $IrCl_3 \cdot 6H_2O$ (75 mg, 0.25 mmol, 1.0 eq.) and ethyl 3',5'-difluoro-3'-(5-(trifluoromethyl)pyridin-2-yl)-[1,1'-biphenyl]-4-carboxylate (**6**) (224 mg, 0.55 mmol, 2.2 eq.) were suspended in a mixture of 2-ethoxyethanol/water (5 mL,

3/1). The mixture was heated and kept at 125 °C under stirring. After 24 h, it was allowed to cool to room temperature and the solvent was removed under vacuo to give the intermediate $[\text{Ir}(\text{C}^{\wedge}\text{N})_2\text{Cl}]_2$ dimer complex, which was directly engaged in the next step without further purification. This complex and picolinic acid (104 mg, 0.75 mmol, 6 eq.) were dissolved in 2-ethoxyethanol (8 mL), and Na_2CO_3 (159 mg, 1.5 mmol, 6 eq.) was added. The solution was heated at 125 °C for 24 h. The solution was allowed to cool to room temperature. After concentration, the residue was purified by flash chromatography on silica gel (CH_2Cl_2 -EtOAc, 75:25) to afford the desired complex **F6** (186 mg, 66%). ^1H NMR (400 MHz, CDCl_3) δ (ppm) 9.11 (s, 1H), 8.41 (d, $J = 7.7$ Hz, 1H), 8.10 – 8.06 (m, 1H), 8.04 (d, $J = 8.3$ Hz, 2H), 7.98 (d, $J = 8.3$ Hz, 3H), 7.95 – 7.86 (m, 4H), 7.57 (t, $J = 6.5$ Hz, 1H), 7.51 – 7.40 (m, 5H), 7.33 (d, $J = 8.0$ Hz, 2H), 4.46 – 4.31 (m, 4H), 1.39 (s, 6H). $^{19}\text{F}\{^1\text{H}\}$ NMR (376 MHz, CDCl_3) δ (ppm) -62.2, -62.8, -107.3 (d, $J = 7.0$ Hz), -121.9 (d, $J = 6.3$ Hz), -122.3 (d, $J = 6.9$ Hz). $^{13}\text{C}\{^1\text{H}\}$ NMR (100 MHz, CDCl_3) δ (ppm) 172.6, 170.1 (d, $J = 4.3$ Hz), 169.9 (d, $J = 4.3$ Hz), 166.2, 166.1, 165.5 (dd, $J = 5.9, 240.5$ Hz), 165.0 (dd, $J = 5.9, 241.1$ Hz), 157.1 (dd, $J = 6.6, 241.8$ Hz), 156.7 (dd, $J = 6.5, 242.4$ Hz), 151.5, 148.4, 146.6 – 146.2 (m), 145.7 – 145.0 (m), 129.3, 135.4 – 134.8 (m), 134.5, 134.0, 130.4 (d, $J = 11.5$ Hz), 130.0 (d, $J = 30.7$ Hz), 129.2, 129.1, 125.8 (d, $J = 34.7$ Hz), 125.4 (d, $J = 34.4$ Hz), 123.1, 133.8, 122.1 (q, $J = 271.6$ Hz), 122.0 (q, $J = 271.6$ Hz), 121.8, 121.4, 120.2 – 119.9 (m), 119.8, 119.1, 108.8 (t, $J = 23.7$ Hz), 108.9 (t, $J = 23.7$ Hz), 61.1, 60.1, 14.3, 14.3. MALDI HRMS for $\text{C}_{48}\text{H}_{31}\text{N}_3\text{O}_6\text{F}_{10}^{193}\text{Ir}$ $[\text{M}+\text{H}]^+$: found 1128.1677, calcd 1128.168. Elemental analysis: calcd (%) for $\text{C}_{48}\text{H}_{30}\text{N}_3\text{O}_6\text{F}_{10}\text{Ir}$ (1126.28): C 51.16, H 2.68, N 3.73; found: C 51.09, H 2.76, N 3.85.

Iridium(III) *bis*[2-(2,4-difluorophenyl)-5-(trifluoromethyl)pyridinato- N,C^2]-4,4'-dimethyl-2,2'-bipyridine hexafluorophosphate (G1): $\text{IrCl}_3 \cdot 6\text{H}_2\text{O}$ (75 mg, 0.25 mmol, 1.0 equiv.) and 2-(2,4-difluorophenyl)-5-(trifluoromethyl)pyridine (**1**) (129 mg, 0.5 mmol, 2 eq.) were suspended in a mixture of 2-ethoxyethanol/water (5 mL, 3/1). The mixture was heated and kept at 125 °C under stirring. After 24 h, it was allowed to cool to room temperature and the solvent was removed under vacuo to give the intermediate $[\text{Ir}(\text{C}^{\wedge}\text{N})_2\text{Cl}]_2$ dimer complex, which was directly engaged in the next step without further purification. The crude mixture of $[\text{Ir}(\text{C}^{\wedge}\text{N})_2\text{Cl}]_2$ (1.0 equiv.) was dissolved in 5 mL of CH_2Cl_2 before addition of 4,4'-dimethyl-2,2'-bipyridine (69 mg, 0.375 mmol, 1.5 equiv.) and AgPF_6 (95 mg, 0.375 mmol, 1.5 equiv.). The resulting solution was stirred at RT over 16 hours away from light. After concentration, the crude mixture was purified by silica column chromatography to afford the

desired complex **G1** (192 mg, 74%). ^1H NMR (400 MHz, Acetone- d_6) δ (ppm) 8.78 (s, 2H), 8.63 (dd, $J = 2.7, 8.8$ Hz, 2H), 8.41 (d, $J = 8.7$ Hz, 2H), 8.11 (d, $J = 5.6$ Hz, 2H), 8.01 (s, 2H), 7.63 (d, $J = 5.7$ Hz, 2H), 6.83 (ddd, $J = 2.3, 9.3, 12.2$ Hz, 2H), 5.97 (dd, $J = 2.3, 8.5$ Hz, 2H), 2.65 (s, 6H). $^{19}\text{F}\{^1\text{H}\}$ NMR (376 MHz, Acetone- d_6) δ (ppm) -63.4, -72.3 (d, $J = 707.6$ Hz), -104.8 (d, $J = 11.9$ Hz), -108.0 (d, $J = 12.8$ Hz). $^{13}\text{C}\{^1\text{H}\}$ NMR (100 MHz, Acetone- d_6) δ (ppm) 167.8 (d, $J = 7.0$ Hz), 164.6 (dd, $J = 12.7, 258.5$ Hz), 162.5 (dd, $J = 13.2, 261.9$ Hz), 155.6, 155.5, 153.3, 150.6, 146.5 (q, $J = 4.7$ Hz), 137.2 (q, $J = 3.4$ Hz), 129.6, 127.1 – 126.6 (m), 126.0, 125.4 (q, $J = 34.6$ Hz), 123.9 (d, $J = 20.9$ Hz), 122.2 (q, $J = 271.7$ Hz), 114.4 (dd, $J = 3.1, 17.9$ Hz), 99.2 (t, $J = 27.1$ Hz), 20.5. MALDI HRMS for $\text{C}_{36}\text{H}_{22}\text{N}_4\text{F}_{10}^{193}\text{Ir} [\text{M}]^+$: found 893.1209, calcd 893.130. Elemental analysis: calcd (%) for $\text{C}_{36}\text{H}_{22}\text{N}_4\text{F}_{16}\text{PIr}$ (1037.77): C 41.67, H 2.14, N 5.40; found: C 41.55, H 2.29, N 5.21.

Iridium(III) *bis*[2-(4'-cyano-2,6-difluoro-[1,1'-biphenyl]-3-yl)-5-(trifluoromethyl)pyridinato-N,C^{2'}]-4,4'-dimethyl-2,2'-bipyridine hexafluorophosphate (G2): $\text{IrCl}_3 \cdot 6\text{H}_2\text{O}$ (75 mg, 0.25 mmol, 1.0 eq.) and 2',6'-difluoro-3'-(5-(trifluoromethyl)pyridin-2-yl)-[1,1'-biphenyl]-4-carbonitrile (**2**) (180 mg, 0.5 mmol, 2 eq.) were suspended in a mixture of 2-ethoxyethanol/water (5 mL, 3/1). The mixture was heated and kept at 125 °C under stirring. After 24 h, it was allowed to cool to room temperature and the solvent was removed under vacuo to give the intermediate $[\text{Ir}(\text{C}^{\wedge}\text{N})_2\text{Cl}]_2$ dimer complex, which was directly engaged in the next step without further purification. The crude mixture of $[\text{Ir}(\text{C}^{\wedge}\text{N})_2\text{Cl}]_2$ (1.0 equiv.) was dissolved in 5 mL of CH_2Cl_2 before addition of 4,4'-dimethyl-2,2'-bipyridine (69 mg, 0.375 mmol, 1.5 equiv.) and AgPF_6 (95 mg, 0.375 mmol, 1.5 equiv.). The resulting solution was stirred at RT over 16 hours away from light. After concentration, the crude mixture was purified by silica column chromatography to afford the desired complex **G2** (217 mg, 70%). ^1H NMR (400 MHz, Acetone- d_6) δ (ppm) 8.81 (s, 2H), 8.69 (dd, $J = 2.6, 8.8$ Hz, 2H), 8.46 (dd, $J = 2.2, 8.8$ Hz, 2H), 8.22 (d, $J = 5.7$ Hz, 2H), 8.07 (d, $J = 2.1$ Hz, 2H), 7.93 (d, $J = 8.3$ Hz, 4H), 7.75 (d, $J = 7.9$ Hz, 4H), 7.63 (d, $J = 5.8$ Hz, 2H), 6.21 (d, $J = 9.4$ Hz, 2H), 2.65 (s, 6H). $^{19}\text{F}\{^1\text{H}\}$ NMR (376 MHz, Acetone- d_6) δ (ppm) -63.5, -72.6 (d, $J = 707.4$ Hz), -109.1 (d, $J = 11.7$ Hz), -112.8 (d, $J = 11.9$ Hz). $^{13}\text{C}\{^1\text{H}\}$ NMR (100 MHz, Acetone- d_6) δ (ppm) 167.7 (d, $J = 7.2$ Hz), 160.9 (dd, $J = 6.8, 259.6$ Hz), 158.8 (dd, $J = 7.4, 263.0$ Hz), 155.6, 155.2 (d, $J = 7.4$ Hz), 153.4, 150.7, 146.2 (q, $J = 4.6$ Hz), 137.4 (m), 134.2, 132.2, 131.3, 129.7, 127.6 (q, $J = 5.5$ Hz), 126.0, 125.7 (q, $J = 34.6$ Hz), 124.3 (d, $J = 22.1$ Hz), 122.12 (q, $J = 271.8$ Hz), 118.2, 115.0 (d, $J = 17.8$ Hz), 112.0 (m),

111.8, 20.5. MALDI HRMS for $C_{50}H_{28}N_6F_{10}^{193}Ir [M]^+$: found 1095.1839, calcd 1095.187. Elemental analysis: calcd (%) for $C_{50}H_{28}N_6F_{16}PIr$ (1239.89): C 48.43, H 2.28, N 6.78; found: C 48.39, H 2.31, N 6.54.

Iridium(III) bis[2-((4'-(ethoxycarbonyl)-2,6-difluoro-[1,1'-biphenyl] 3-yl)-5-(trifluoromethyl)pyridinato-N,C^{2'}]-4,4'-dimethyl-2,2'-bipyridine hexafluorophosphate (G3): $IrCl_3 \cdot 6H_2O$ (75 mg, 0.25 mmol, 1.0 eq.) and ethyl 2',6'-difluoro-3'-(5-(trifluoromethyl)pyridin-2-yl)-[1,1'-biphenyl]-4-carboxylate (**3**) (203 mg, 0.5 mmol, 2 eq.) were suspended in a mixture of 2-ethoxyethanol/water (5 mL, 3/1). The mixture was heated and kept at 125 °C under stirring. After 24 h, it was allowed to cool to room temperature and the solvent was removed under vacuo to give the intermediate $[Ir(C^{\wedge}N)_2Cl]_2$ dimer complex, which was directly engaged in the next step without further purification. The crude mixture of $[Ir(C^{\wedge}N)_2Cl]_2$ (1.0 equiv.) was dissolved in 5 mL of CH_2Cl_2 before addition of 4,4'-dimethyl-2,2'-bipyridine (69 mg, 0.375 mmol, 1.5 equiv.) and $AgPF_6$ (95 mg, 0.375 mmol, 1.5 equiv.). The resulting solution was stirred at RT over 16 hours away from light. After concentration, the crude mixture was purified by silica column chromatography to afford the desired complex **G3** (226 mg, 68%). 1H NMR (400 MHz, $CDCl_3$) δ (ppm) 8.67 (s, 2H), 8.59 – 8.51 (m, 2H), 8.11 (dd, $J = 8.3, 13.2$ Hz, 6H), 7.92 (d, $J = 5.7$ Hz, 2H), 7.66 (s, 2H), 7.58 (d, $J = 8.0$ Hz, 4H), 7.48 (d, $J = 5.7$ Hz, 2H), 5.85 (d, $J = 8.8$ Hz, 2H), 4.41 (q, $J = 7.1$ Hz, 4H), 2.65 (s, 6H), 1.42 (t, $J = 7.1$ Hz, 6H). $^{19}F\{^1H\}$ NMR (376 MHz, $CDCl_3$) δ (ppm) -62.8, -72.6 (d, $J = 712.5$ Hz), -105.4 (d, $J = 13.5$ Hz), -110.5 (d, $J = 14.2$ Hz). $^{13}C\{^1H\}$ NMR (100 MHz, $CDCl_3$) δ (ppm) 168.0 (d, $J = 7.1$ Hz), 166.2, 161.5 (dd, $J = 7.0, 262.5$ Hz), 159.2 (dd, $J = 7.0, 264.4$ Hz), 154.9, 154.5, 153.5 (d, $J = 7.4$ Hz), 149.6, 148.7, 144.9 (q, $J = 5.0$ Hz), 136.7, 133.5, 130.3, 130.2, 130.0, 129.4, 126.8, 126.4 (q, $J = 35.0$ Hz), 124.1 (d, $J = 22.7$ Hz), 123.5 (q, $J = 272.1$ Hz), 122.9, 120.2, 114.5 (d, $J = 19.1$ Hz), 113.3 (t, $J = 19.8$ Hz), 61.1, 29.7, 14.3. MALDI HRMS for $C_{54}H_{38}N_4O_4F_{10}^{193}Ir [M]^+$: found 1189.2357, calcd 1189.232. Elemental analysis: calcd (%) for $C_{54}H_{38}N_4O_4F_{16}PIr$ (1334.09): C 48.62, H 2.87, N 4.20; found: C 48.69, H 2.61, N 4.42.

Iridium(III) bis[2-(4'-acetyl-2,6-difluoro-[1,1'-biphenyl]-3-yl)-5-(trifluoromethyl)pyridinato-N,C^{2'}]-4,4'-dimethyl-2,2'-bipyridine hexafluorophosphate

(G4): IrCl₃.6H₂O (75 mg, 0.25 mmol, 1.0 eq.) and ethyl 1-(2',6'-difluoro-3'-(5-(trifluoromethyl)pyridin-2-yl)-[1,1'-biphenyl]-4-yl)ethan-1-one (**4**) (138 mg, 0.5 mmol, 2 eq.) were suspended in a mixture of 2-ethoxyethanol/water (5 mL, 3/1). The mixture was heated and kept at 125 °C under stirring. After 24 h, it was allowed to cool to room temperature and the solvent was removed under vacuo to give the intermediate [Ir(C[^]N)₂Cl]₂ dimer complex, which was directly engaged in the next step without further purification. The crude mixture of [Ir(C[^]N)₂Cl]₂ (1.0 equiv.) was dissolved in 5 mL of CH₂Cl₂ before addition of 4,4'-dimethyl-2,2'-bipyridine (69 mg, 0.375 mmol, 1.5 equiv.) and AgPF₆ (95 mg, 0.375 mmol, 1.5 equiv.). The resulting solution was stirred at RT over 16 hours away from light. After concentration, the crude mixture was purified by silica column chromatography to afford the desired complex **G4** (204 mg, 64%). ¹H NMR (400 MHz, Acetone-*d*₆) δ (ppm) 8.81 (s, 2H), 8.74 – 8.66 (m, 2H), 8.48 – 8.41 (m, 2H), 8.26 – 8.21 (m, 2H), 8.12 (d, *J* = 8.2 Hz, 2H), 8.09 – 8.06 (m, 2H), 7.69 – 7.63 (m, 4H), 7.60 (d, *J* = 8.2 Hz, 2H), 7.49 (d, *J* = 8.2 Hz, 2H), 6.24 – 6.11 (m, 2H), 2.66 (s, 6H), 2.65 (s, 6H). ¹⁹F{¹H} NMR (376 MHz, CDCl₃) δ (ppm) -63.5, -72.5 (d, *J* = 707.4 Hz), -108.7 (d, *J* = 12.2 Hz), -112.6 (d, *J* = 12.8 Hz). ¹³C{¹H} NMR (100 MHz, CDCl₃) δ (ppm) 196.7, 167.9 (d, *J* = 7.7 Hz), 161.1 (dd, *J* = 6.7, 259.2 Hz), 159.1 (md, *J* = 237.7 Hz), 155.7, 154.5 (d, *J* = 7.7 Hz), 153.3 (q, *J* = 3.0 Hz), 150.7, 150.6, 146.2 (m), 137.3, 136.7, 133.9, 130.6, 129.7, 128.1, 128.4 (q, *J* = 35.9 Hz), 127.4 (m), 126.0, 125.2, 124.2 (md, *J* = 22.5 Hz), 122.2 (q, *J* = 271.7 Hz), 114.9 (md, *J* = 16.6 Hz), 108.3, 25.8, 20.5. MALDI HRMS for C₅₂H₃₄N₄O₂F₁₀¹⁹³Ir [M]⁺: found 1129.2146, calcd 1129.218. Elemental analysis: calcd (%) for C₅₂H₃₄N₄O₂F₁₆PIr (1274.04): C 49.02, H 2.69, N 4.40; found: C 49.17, H 2.86, N 4.20.

Iridium(III) bis[2-(3,5-difluorophenyl)-5-(trifluoromethyl)pyridinato-N,C^{2'}]-4,4'-dimethyl-2,2'-bipyridine hexafluorophosphate (G5): IrCl₃.6H₂O (75 mg, 0.25 mmol, 1.0 equiv.) and 2-(3,5-difluorophenyl)-5-(trifluoromethyl)pyridine (**5**) (129 mg, 0.5 mmol, 2 eq.) were suspended in a mixture of 2-ethoxyethanol/water (5 mL, 3/1). The mixture was heated and kept at 125 °C under stirring. After 24 h, it was allowed to cool to room temperature and the solvent was removed under vacuo to give the intermediate [Ir(C[^]N)₂Cl]₂ dimer complex, which was directly engaged in the next step without further purification. The crude mixture of [Ir(C[^]N)₂Cl]₂ (1.0 equiv.) was dissolved in 5 mL of CH₂Cl₂ before addition of 4,4'-dimethyl-2,2'-bipyridine (69 mg, 0.375 mmol, 1.5 equiv.) and AgPF₆ (95 mg, 0.375 mmol,

1.5 equiv.). The resulting solution was stirred at RT over 16 hours away from light. After concentration, the crude mixture was purified by silica column chromatography to afford the desired complex **G5** (181 mg, 70%). ^1H NMR (400 MHz, Acetone- d_6) δ (ppm) 8.79 (s, 2H), 8.57 (d, $J = 8.6$ Hz, 2H), 8.37 (dd, $J = 2.1, 8.7$ Hz, 2H), 8.14 (d, $J = 5.7$ Hz, 2H), 7.95 – 7.86 (m, 4H), 7.65 (d, $J = 5.6$ Hz, 2H), 6.69 (td, $J = 2.4, 9.4$ Hz, 2H), 2.66 (s, 6H). $^{19}\text{F}\{^1\text{H}\}$ NMR (376 MHz, Acetone- d_6) δ (ppm) -63.4, -72.2 (d, $J = 708.3$ Hz), -102.5 (d, $J = 7.6$ Hz), -118.8 (d, $J = 7.8$ Hz). $^{13}\text{C}\{^1\text{H}\}$ NMR (100 MHz, Acetone- d_6) δ (ppm) 170.7 (d, $J = 4.6$ Hz), 168.4 (dd, $J = 11.2, 238.9$ Hz), 160.5 (dd, $J = 12.3, 240.1$ Hz), 155.9, 153.4, 150.3, 146.7 (dd, $J = 9.2, 17.6$ Hz), 146.4 (q, $J = 4.9$ Hz), 136.4 (q, $J = 3.4$ Hz), 129.9, 126.2, 125.6 (q, $J = 34.3$ Hz), 124.7 (dd, $J = 3.0, 36.4$ Hz), 122.2 (q, $J = 271.8$ Hz), 121.1, 109.6 (dd, $J = 3.8, 22.3$ Hz), 106.5 (dd, $J = 24.9, 32.3$ Hz), 20.5. MALDI HRMS for $\text{C}_{36}\text{H}_{22}\text{N}_4\text{F}_{10}^{193}\text{Ir} [\text{M}]^+$: found 893.1209, calcd 893.130. Elemental analysis: calcd (%) for $\text{C}_{36}\text{H}_{22}\text{N}_4\text{F}_{16}\text{PIr}$ (1037.77): C 41.67, H 2.14, N 5.40; found: C 41.84, H 2.31, N 5.67.

Iridium(III) *bis*[2-((4'-(ethoxycarbonyl)-3,5-difluoro-[1,1'-biphenyl]-3-yl)-5-(trifluoromethyl)pyridinato- $\text{N},\text{C}^{2'}$)]-4,4'-dimethyl-2,2'-bipyridine hexafluorophosphate (**G6**): $\text{IrCl}_3 \cdot 6\text{H}_2\text{O}$ (75 mg, 0.25 mmol, 1.0 eq.) and ethyl 3',5'-difluoro-3'-(5-(trifluoromethyl)pyridin-2-yl)-[1,1'-biphenyl]-4-carboxylate (**6**) (203 mg, 0.5 mmol, 2 eq.) were suspended in a mixture of 2-ethoxyethanol/water (5 mL, 3/1). The mixture was heated and kept at 125 °C under stirring. After 24 h, it was allowed to cool to room temperature and the solvent was removed under vacuo to give the intermediate $[\text{Ir}(\text{C}^{\wedge}\text{N})_2\text{Cl}]_2$ dimer complex, which was directly engaged in the next step without further purification. The crude mixture of $[\text{Ir}(\text{C}^{\wedge}\text{N})_2\text{Cl}]_2$ (1.0 equiv.) was dissolved in 5 mL of CH_2Cl_2 before addition of 4,4'-dimethyl-2,2'-bipyridine (69 mg, 0.375 mmol, 1.5 equiv.) and AgPF_6 (95 mg, 0.375 mmol, 1.5 equiv.). The resulting solution was stirred at RT over 16 hours away from light. After concentration, the crude mixture was purified by silica column chromatography to afford the desired complex **G6** (213 mg, 64%). ^1H NMR (400 MHz, CD_2Cl_2) δ (ppm) 8.47 (s, 2H), 8.06 (d, $J = 8.2$ Hz, 8H), 8.02 (d, $J = 5.6$ Hz, 2H), 7.68 – 7.60 (m, 4H), 7.46 (d, $J = 7.2$ Hz, 6H), 4.38 (q, $J = 7.1$ Hz, 4H), 2.71 (s, 6H), 1.41 (t, $J = 7.1$ Hz, 6H). $^{19}\text{F}\{^1\text{H}\}$ NMR (376 MHz, CD_2Cl_2) δ (ppm) -63.3, -73.0 (d, $J = 710.9$ Hz), -106.4, -120.9. $^{13}\text{C}\{^1\text{H}\}$ NMR (100 MHz, CD_2Cl_2) δ (ppm) 170.1, 165.9, 174.2 (dd, $J = 7.0, 246.7$), 157.6 (dd, $J = 7.0, 246.7$), 155.1, 154.2, 149.9, 145.6 (d, $J = 4.6$ Hz), 136.0 (q, $J = 3.8$ Hz), 133.7, 130.4, 130.3, 130.1, 129.1, 126.2, 120.5, 124.4 (d, $J = 2.6$ Hz), 124.0 (d, $J = 3.5$ Hz), 121.8 (q, $J = 274.1$ Hz),

120.5, 109.7 (dd, $J = 3.7, 24.0$ Hz), 61.1, 21.4, 14.1. MALDI HRMS for $C_{54}H_{38}N_4O_4F_{10}^{193}Ir$ $[M]^+$: found 1189.2357, calcd 1189.239. Elemental analysis: calcd (%) for $C_{54}H_{38}N_4O_4F_{16}PIr$ (1334.09): C 48.62, H 2.87, N 4.20; found: C 48.45, H 2.90, N 4.21.

ASSOCIATED CONTENT

Crystallographic information file for **F2** (CCDC 1964093) (CIF)

Crystallographic information file for **F5** (CCDC 1964103) (CIF)

Crystallographic information file for **F6** (CCDC 1964108) (CIF)

Crystallographic information file for **G3** (CCDC 1964137) (CIF)

Crystallographic information file for **G5** (CCDC 1964149) (CIF)

Experimental details on cyclic voltammetry, X-ray; 1H , ^{19}F and ^{13}C NMR spectra, (PDF)

Corresponding Author

*yunchi@cityu.edu.hk, *veronique.guerchais@univ-rennes1.fr; *henri.doucet@univ-rennes1.fr; *jean-francois.soule@univ-rennes1.fr

ACKNOWLEDGMENT

R.B. is grateful to “Université Mohamed Premier, Oujda, Morocco” for providing financial support. We thank CNRS (I.E.A. Hong Kong) and UR1 for providing financial support.

REFERENCES

- (a) You, Y.; Park, S. Y., Phosphorescent Iridium(III) Complexes: Toward High Phosphorescence Quantum Efficiency through Ligand Control. *Dalton Trans.* **2009**, 1267-1282; (b) Chi, Y.; Chou, P.-T., Transition-Metal Phosphors with Cyclometalating Ligands: Fundamentals and Applications. *Chem. Soc. Rev.* **2010**, *39*, 638-655; (c) Zhao, Q.; Li, F.; Huang, C., Phosphorescent Chemosensors Based on Heavy-Metal Complexes. *Chem. Soc. Rev.* **2010**, *39*, 3007-3030; (d) You, Y.; Nam, W., Photofunctional Triplet Excited States of Cyclometalated Ir(III) Complexes: Beyond Electroluminescence. *Chem. Soc. Rev.* **2012**, *41*, 7061-7084; (e) *Archetypal Iridium(III) Compounds for Optoelectronic and Photonic Applications*. Eli Zysman-Colman ed.; John Wiley & Sons Ltd.: Chichester, 2017; (f) Chi, Y.; Chang, T.-K.; Ganesan, P.; Rajakannu, P., Emissive bis-Tridentate Ir(III) Metal Complexes: Tactics, Photophysics and Applications. *Coord. Chem. Rev.* **2017**, *346*, 91-100; (g) Haghghatbin, M. A.; Laird, S. E.; Hogan, C. F., Electrochemiluminescence of Cyclometalated Iridium (III) Complexes. *Curr. Opin. Electrochem.* **2018**, *7*, 216-223; (h)

Chi, Y.; Wang, S. F.; Ganesan, P., Emissive Iridium(III) Complexes with Phosphorous-Containing Ancillary. *Chem. Rec.* **2019**, *19*, 1644-1666; (i) Feng, Z.; Sun, Y.; Yang, X.; Zhou, G., Novel Emission Color-Tuning Strategies in Heteroleptic Phosphorescent Ir(III) and Pt(II) Complexes. *Chem. Rec.* **2019**, *19*, 1710-1728.

2. Duan, J. P.; Sun, P. P.; Cheng, C. H., New Iridium Complexes as Highly Efficient Orange–Red Emitters in Organic Light-Emitting Diodes. *Adv. Mater.* **2003**, *15*, 224-228.

3. (a) *Highly Efficient OLEDs with Phosphorescent Materials*. Yersin, Hartmut ed.; John Wiley & Sons: Weinheim, 2008; (b) He, L.; Duan, L.; Qiao, J.; Wang, R.; Wei, P.; Wang, L.; Qiu, Y., Blue-Emitting Cationic Iridium Complexes with 2-(1H-Pyrazol-1-yl)pyridine as the Ancillary Ligand for Efficient Light-Emitting Electrochemical Cells. *Adv. Funct. Mater.* **2008**, *18*, 2123-2131; (c) Ulbricht, C.; Beyer, B.; Friebe, C.; Winter, A.; Schubert, U. S., Recent Developments in the Application of Phosphorescent Iridium(III) Complex Systems. *Adv. Mater.* **2009**, *21*, 4418-4441; (d) Costa, R. D.; Ortí, E.; Bolink, H. J.; Graber, S.; Schaffner, S.; Neuburger, M.; Housecroft, C. E.; Constable, E. C., Archetype Cationic Iridium Complexes and Their Use in Solid-State Light-Emitting Electrochemical Cells. *Adv. Funct. Mater.* **2009**, *19*, 3456-3463; (e) Yersin, H.; Rausch, A. F.; Czerwieniec, R.; Hofbeck, T.; Fischer, T., The Triplet State of Organo-Transition Metal Compounds. Triplet Harvesting and Singlet Harvesting for Efficient OLEDs. *Coord. Chem. Rev.* **2011**, *255*, 2622-2652; (f) Costa, R. D.; Ortí, E.; Bolink, H. J.; Monti, F.; Accorsi, G.; Armaroli, N., Luminescent Ionic Transition-Metal Complexes for Light-Emitting Electrochemical Cells. *Angew. Chem. Int. Ed.* **2012**, *51*, 8178-8211; (g) Gildea, L. F.; Williams, J. A. G., 3 - Iridium and Platinum Complexes for OLEDs. In *Organic Light-Emitting Diodes (OLEDs)*, Buckley, A., Ed. Woodhead Publishing: 2013; pp 77-113; (h) Martir, D. R.; Momblona, C.; Pertegás, A.; Cordes, D. B.; Slawin, A. M. Z.; Bolink, H. J.; Zysman-Colman, E., Chiral Iridium(III) Complexes in Light-Emitting Electrochemical Cells: Exploring the Impact of Stereochemistry on the Photophysical Properties and Device Performances. *ACS Appl. Mater. Interfaces* **2016**, *8*, 33907-33915.

4. (a) Tamayo, A. B.; Garon, S.; Sajoto, T.; Djurovich, P. I.; Tsyba, I. M.; Bau, R.; Thompson, M. E., Cationic Bis-cyclometalated Iridium(III) Diimine Complexes and Their Use in Efficient Blue, Green, and Red Electroluminescent Devices. *Inorg. Chem.* **2005**, *44*, 8723-8732; (b) He, L.; Duan, L.; Qiao, J.; Dong, G.; Wang, L.; Qiu, Y., Highly Efficient Blue-Green and White Light-Emitting Electrochemical Cells Based on a Cationic Iridium Complex with a Bulky Side Group. *Chem. Mater.* **2010**, *22*, 3535-3542; (c) Kessler, F.; Costa, R. D.; Di Censo, D.; Scopelliti, R.; Ortí, E.; Bolink, H. J.; Meier, S.; Sarfert, W.;

- Grätzel, M.; Nazeeruddin, M. K.; Baranoff, E., Near-UV to Red-Emitting Charged bis-Cyclometalated Iridium(III) Complexes for Light-Emitting Electrochemical Cells. *Dalton Trans.* **2012**, *41*, 180-191; (d) Skórka, Ł.; Filapek, M.; Zur, L.; Małecki, J. G.; Pisarski, W.; Olejnik, M.; Danikiewicz, W.; Krompiec, S., Highly Phosphorescent Cyclometalated Iridium(III) Complexes for Optoelectronic Applications: Fine Tuning of the Emission Wavelength through Ancillary Ligands. *J. Phys. Chem. C* **2016**, *120*, 7284-7294; (e) Chau, N.-Y.; Ho, P.-Y.; Ho, C.-L.; Ma, D.; Wong, W.-Y., Color-Tunable Thiazole-Based Iridium(III) Complexes: Synthesis, Characterization and their OLED Applications. *J. Organomet. Chem.* **2017**, *829*, 92-100; (f) Lai, P.-N.; Teets, T. S., Ancillary Ligand Effects on Red-Emitting Cyclometalated Iridium Complexes. *Chem. Eur. J.* **2019**, *25*, 6026-6037.
5. (a) Su, S.-J.; Chiba, T.; Takeda, T.; Kido, J., Pyridine-Containing Triphenylbenzene Derivatives with High Electron Mobility for Highly Efficient Phosphorescent OLEDs. *Adv. Mater.* **2008**, *20*, 2125-2130; (b) Sasabe, H.; Gonmori, E.; Chiba, T.; Li, Y.-J.; Tanaka, D.; Su, S.-J.; Takeda, T.; Pu, Y.-J.; Nakayama, K.-i.; Kido, J., Wide-Energy-Gap Electron-Transport Materials Containing 3,5-Dipyridylphenyl Moieties for an Ultra High Efficiency Blue Organic Light-Emitting Device. *Chem. Mater.* **2008**, *20*, 5951-5953; (c) Xiao, L.; Su, S.-J.; Agata, Y.; Lan, H.; Kido, J., Nearly 100% Internal Quantum Efficiency in an Organic Blue-Light Electrophosphorescent Device Using a Weak Electron Transporting Material with a Wide Energy Gap. *Adv. Mater.* **2009**, *21*, 1271-1274; (d) Bin, J.-K.; Cho, N.-S.; Hong, J.-I., New Host Material for High-Performance Blue Phosphorescent Organic Electroluminescent Devices. *Adv. Mater.* **2012**, *24*, 2911-2915; (e) Baranoff, E.; Curchod, B. F. E., Flrpic: Archetypal Blue Phosphorescent Emitter for Electroluminescence. *Dalton Trans.* **2015**, *44*, 8318-8329.
6. Lee, S.; Kim, S.-O.; Shin, H.; Yun, H.-J.; Yang, K.; Kwon, S.-K.; Kim, J.-J.; Kim, Y.-H., Deep-Blue Phosphorescence from Perfluoro Carbonyl-Substituted Iridium Complexes. *J. Am. Chem. Soc.* **2013**, *135*, 14321-14328.
7. Okamura, N.; Nakamura, T.; Yagi, S.; Maeda, T.; Nakazumi, H.; Fujiwara, H.; Koseki, S., Novel *bis*- and *tris*-Cyclometalated Iridium(III) Complexes Bearing a Benzoyl Group on Each Fluorinated 2-Phenylpyridinate Ligand Aimed at Development of Blue Phosphorescent Materials for OLED. *RSC Adv.* **2016**, *6*, 51435-51445.
8. Yu, H.; Liu, C.; Lv, X.; Xiu, J.; Zhao, J., Effect of Substituents on Properties of Diphenylphosphoryl-Substituted bis-Cyclometalated Ir(III) Complexes with a Picolinic Acid as Ancillary Ligand. *Dyes Pigm.* **2017**, *145*, 136-143.

9. Yun, S.-J.; Jeon, J.; Jin, S.-H.; Kang, S. K.; Kim, Y.-I., Synthesis, Structure, and OLEDs Application of Cyclometalated Iridium(III) Complexes Utilizing Substituted 2-Phenylpyridine. *Bull. Korean Chem. Soc.* **2017**, *38*, 788-794.
10. (a) Kozhevnikov, V. N.; Zheng, Y.; Clough, M.; Al-Attar, H. A.; Griffiths, G. C.; Abdullah, K.; Raisys, S.; Jankus, V.; Bryce, M. R.; Monkman, A. P., Cyclometalated Ir(III) Complexes for High-Efficiency Solution-Processable Blue PhOLEDs. *Chem. Mater.* **2013**, *25*, 2352-2358; (b) Rota Martir, D.; Hedley, G. J.; Cordes, D. B.; Slawin, A. M. Z.; Escudero, D.; Jacquemin, D.; Kosikova, T.; Philp, D.; Dawson, D. M.; Ashbrook, S. E.; Samuel, I. D. W.; Zysman-Colman, E., Exploring the Self-Assembly and Energy Transfer of Dynamic Supramolecular Iridium-Porphyrin Systems. *Dalton Trans.* **2016**, *45*, 17195-17205; (c) Suhr, K. J.; Bastatas, L. D.; Shen, Y.; Mitchell, L. A.; Holliday, B. J.; Slinker, J. D., Enhanced Luminance of Electrochemical Cells with a Rationally Designed Ionic Iridium Complex and an Ionic Additive. *ACS Appl. Mater. Interfaces* **2016**, *8*, 8888-8892; (d) Rota Martir, D.; Bansal, A. K.; Di Mascio, V.; Cordes, D. B.; Henwood, A. F.; Slawin, A. M. Z.; Kamer, P. C. J.; Martínez-Sarti, L.; Pertegás, A.; Bolink, H. J.; Samuel, I. D. W.; Zysman-Colman, E., Enhancing the Photoluminescence Quantum Yields of Blue-Emitting Cationic Iridium(III) Complexes Bearing Bisphosphine Ligands. *Inorg. Chem. Front.* **2016**, *3*, 218-235; (e) Hierlinger, C.; Trzop, E.; Toupet, L.; Ávila, J.; La-Placa, M.-G.; Bolink, H. J.; Guerschais, V.; Zysman-Colman, E., Impact of the Use of Sterically Congested Ir(III) Complexes on the Performance of Light-Emitting Electrochemical Cells. *J. Mater. Chem. C* **2018**, *6*, 6385-6397.
11. Boyaala, R.; Touzani, R.; Roisnel, T.; Dorcet, V.; Caytan, E.; Jacquemin, D.; Boixel, J.; Guerschais, V.; Doucet, H.; Soulé, J.-F., Catalyst-Controlled Regiodivergent C–H Arylation Site of Fluorinated 2-Arylpyridine Derivatives: Application to Luminescent Iridium(III) Complexes. *ACS Catal.* **2019**, *9*, 1320-1328.
12. Bünzli, A. M.; Constable, E. C.; Housecroft, C. E.; Prescimone, A.; Zampese, J. A.; Longo, G.; Gil-Escrig, L.; Pertegás, A.; Ortí, E.; Bolink, H. J., Exceptionally Long-Lived Light-Emitting Electrochemical Cells: Multiple Intra-Cation π -Stacking Interactions in $[\text{Ir}(\text{C}^{\wedge}\text{N})_2(\text{N}^{\wedge}\text{N})][\text{PF}_6]$ Emitters. *Chem. Sci.* **2015**, *6*, 2843-2852.
13. (a) Ackermann, L.; Vicente, R.; Kapdi, A. R., Transition-Metal-Catalyzed Direct Arylation of (Hetero)Arenes by C–H Bond Cleavage. *Angew. Chem. Int. Ed.* **2009**, *48*, 9792-9826; (b) Chen, X.; Engle, K. M.; Wang, D.-H.; Yu, J.-Q., Palladium(II)-Catalyzed C–H Activation/C–C Cross-Coupling Reactions: Versatility and Practicality. *Angew. Chem. Int. Ed.* **2009**, *48*, 5094-5115; (c) Satoh, T.; Miura, M., Transition-Metal-Catalyzed

Regioselective Arylation and Vinylation of Carboxylic Acids. *Synthesis* **2010**, 3395-3409; (d) Hirano, K.; Miura, M., Recent Advances in Copper-mediated Direct Biaryl Coupling. *Chem. Lett.* **2015**, *44*, 878-873; (e) Sinha, S. K.; Zanoni, G.; Maiti, D., Natural Product Synthesis by C–H Activation. *Asian J. Org. Chem.* **2018**, *7*, 1178-1192; (f) Hagui, W.; Doucet, H.; Soulé, J.-F., Application of Palladium-Catalyzed C(sp²)–H Bond Arylation to the Synthesis of Polycyclic (Hetero)Aromatics. *Chem* **2019**, *5*, 2006-2078.

14. He, M.; Soulé, J.-F.; Doucet, H., Synthesis of (Poly)fluorobiphenyls through Metal-catalyzed C-H Bond Activation/Arylation of (Poly)fluorobenzene Derivatives. *ChemCatChem* **2014**, *6*, 1824-1859.

15. (a) Lafrance, M.; Rowley, C. N.; Woo, T. K.; Fagnou, K., Catalytic Intermolecular Direct Arylation of Perfluorobenzenes. *J. Am. Chem. Soc.* **2006**, *128*, 8754-8756; (b) Garcia-Cuadrado, D.; de Mendoza, P.; Braga, A. A. C.; Maseras, F.; Echavarren, A. M., Proton-Abstraction Mechanism in the Palladium-Catalyzed Intramolecular Arylation: Substituent Effects. *J. Am. Chem. Soc.* **2007**, *129*, 6880-6886; (c) Ackermann, L.; Fenner, S., Direct Arylations of Electron-Deficient (Hetero)arenes with Aryl or Alkenyl Tosylates and Mesylates. *Chem. Commun.* **2011**, *47*, 430-432; (d) Bernhammer, J. C.; Huynh, H. V., Pyrazolin-5-ylidene Palladium(II) Complexes: Synthesis, Characterization, and Application in the Direct Arylation of Pentafluorobenzene. *Organometallics* **2012**, *31*, 5121-5130; (e) He, M.; Soulé, J.-F.; Doucet, H., Reactivity of Para-Substituted Fluorobenzenes in Palladium-catalyzed Intermolecular Direct Arylations. *ChemCatChem* **2015**, *7*, 2130-2140; (f) Obligacion, J. V.; Bezdek, M. J.; Chirik, P. J., C(sp²)–H Borylation of Fluorinated Arenes Using an Air-Stable Cobalt Precatalyst: Electronically Enhanced Site Selectivity Enables Synthetic Opportunities. *J. Am. Chem. Soc.* **2017**, *139*, 2825-2832.

16. Wang, Y.-N.; Guo, X.-Q.; Zhu, X.-H.; Zhong, R.; Cai, L.-H.; Hou, X.-F., Pd(OAc)₂-Catalyzed Direct Arylation of Electron-Deficient Arenes Without Ligands or With Monoprotected Amino Acid Assistance. *Chem. Commun.* **2012**, *48*, 10437-10439.

17. Lowry, M. S.; Goldsmith, J. I.; Slinker, J. D.; Rohl, R.; Pascal, R. A.; Malliaras, G. G.; Bernhard, S., Single-Layer Electroluminescent Devices and Photoinduced Hydrogen Production from an Ionic Iridium(III) Complex. *Chem. Mater.* **2005**, *17*, 5712-5719.

18. Leung, C. F.; Cheng, S. C.; Yang, Y.; Xiang, J.; Yiu, S. M.; Ko, C. C.; Lau, T. C., Efficient Photocatalytic Water Reduction by a Cobalt(II) Tripodal Iminopyridine Complex. *Catal. Sci. Technol.* **2018**, *8*, 307-313.

19. Hsu, L.-Y.; Chen, D.-G.; Liu, S.-H.; Chiu, T.-Y.; Chang, C.-H.; Jen, A. K. Y.; Chou, P.-T.; Chi, Y., Roles of Ancillary Chelates and Overall Charges of Bis-tridentate Ir(III) Phosphors for OLED Applications. *ACS Appl. Mater. Interfaces* **2020**, *12*, 1084-1093.
20. Cantat, T.; Génin, E.; Giroud, C.; Meyer, G.; Jutand, A., Structural and kinetic effects of chloride ions in the palladium-catalyzed allylic substitutions. *J. Organomet. Chem.* **2003**, *687*, 365-376.
21. Luo, J.; Zhang, J., Donor–Acceptor Fluorophores for Visible-Light-Promoted Organic Synthesis: Photoredox/Ni Dual Catalytic C(sp³)–C(sp²) Cross-Coupling. *ACS Catal.* **2016**, *6*, 873-877.